University of Stavanger

Faculty of Science and Technology

MASTER'S THESIS

Study program/ Specialization: Master in Offshore Engineering/ Environmental Technology	Spring semester, 2011 Open
Writer: Astrid Lone	…… (Writer's signature)
Faculty supervisor: Malcolm A. Kelland External supervisor(s):	
Title of thesis: "ESTABLISHING A NEW HIGH PRESSURE STEEL MULTI-CELL ROCKER RIG FOR KINETIC HYDRATE INHIBITOR TESTING"	
Credits (ECTS): 30	
Key words: Gas hydrates Low dosage hydrate inhibitors High pressure rocker rig Kinetic hydrate inhibitor	Pages: 102 + 3 + enclosure: 2 Stavanger, 14.07.11 Date/year

Master Thesis in Environmental Technology – Offshore 2011

Establishing a new high pressure steel multi-cell Rocker Rig for kinetic hydrate inhibitor testing

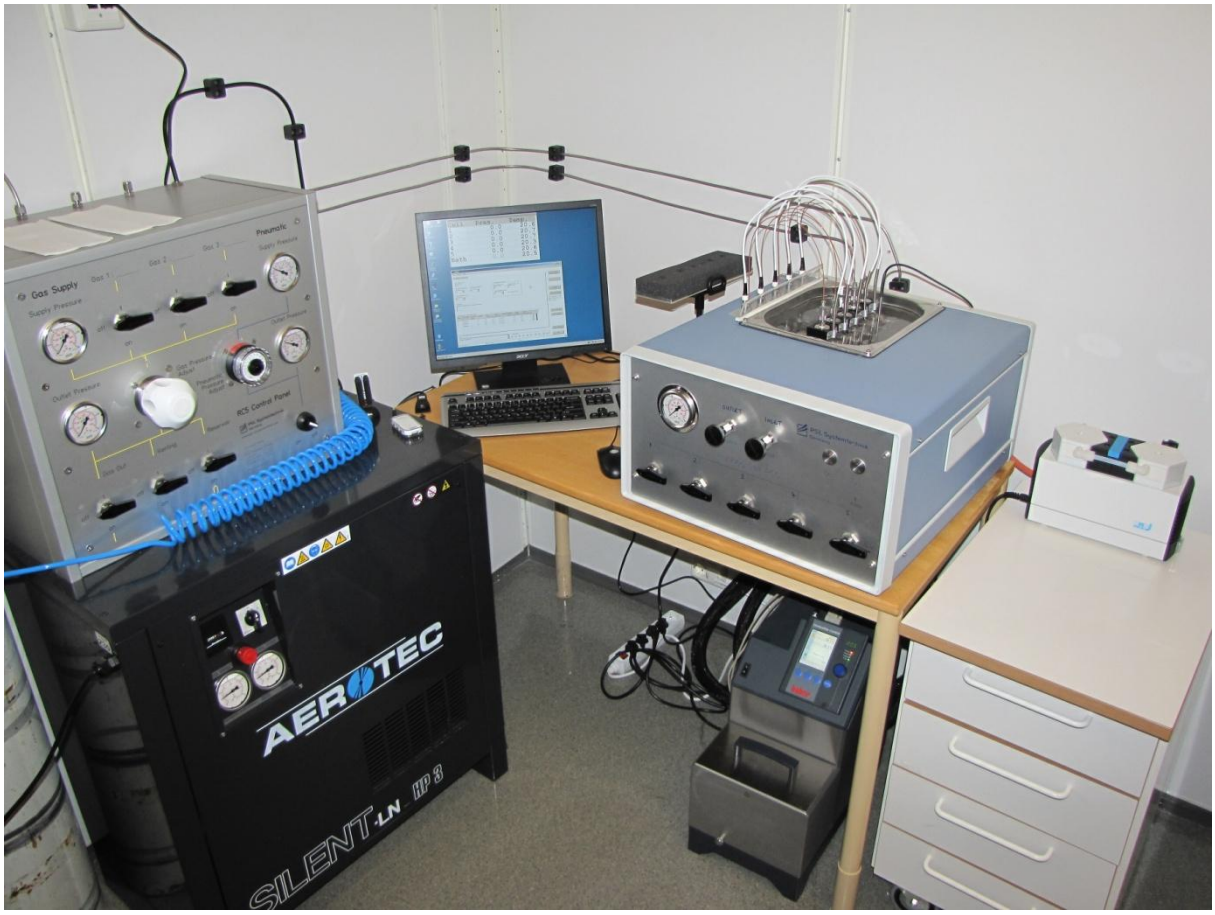

The set-up of the Rocking Cell 5

Content

Acknowledgements

Most importantly, I would like to thank my supervisor Malcolm A. Kelland at the University of Stavanger, Department of Mathematics and Natural Science, for great support and guidance while working on the thesis. I would also like to thank PhD student Pei Cheng Chua for her assistance in the lab.

Finally I would like to thank my family, especially Joar, for letting me go to the lab every day knowing that our baby is in the best hands.

Thanks!

Abstract

Low dosage hydrate inhibitors (LDHIs) is a cost-effective alternative to traditional thermodynamic inhibitors (THIs), like methanol and glycols, to prevent the occurrence of natural gas hydrates in gas and oilfield operations. One class of LDHIs is the kinetic hydrate inhibitors (KHIs). KHIs have been used commercially in the field for the last 15 years, and the development and search for new KHIs is an ongoing process.

This report describes how high pressure rocker rigs can be used to rank KHIs based on their effectiveness and efficiency under different conditions.

The high pressure rocker rig used for this thesis was delivered at the end of November, and the experiments started on December 1st. The last experiment took place May 2nd. The Rocking Cell RC5 has five cells that provide five individual results from every experiment. This makes it a very time-effective rocker rig compared to, say, autoclaves, where one normally only obtains one result per day. Since the start-up with the rocker rig in December there have been no major problems, and so it has been a very reliable piece of equipment.

A procedure for the Rocking Cell RC5 has been established. Experiments are run using a constant cooling method and an isothermal method. The reproducibility was found to be best using the constant cooling method. Compared to alternative apparatus the reproducibility has proven to be very good. Reported information from experiences using autoclaves, say that the scattering in hold time using non-precursor methods is usually 30-40% on either side of average of series. Using the constant cooling method the scattering in hold time is found to be within 4.4%.

The main focus of these thesis has been testing four already known KHIs; Luvicap 55W, Luvicap EG, Inhibex 101 and Inhibex 501. The chemicals are ranked based on how well they inhibit the gas hydrate formation. Inhibex 101 was found to be the best one, both using the constant cooling method and the isothermal method.

Since there are no thorough published studies available on the use of rocker rigs to rank the performance of KHIs, the results cannot be compared to experiments from other groups. For some results, more tests should therefore be run to check the validity of the results.

1. Introduction

The formations of gas hydrates in pipes and wells are a big challenge in offshore drilling processes (Carroll 2009). These formations can lead to both operational and safety problems. The prevention of gas hydrate plugging of flowlines is considered one of the main production issues to deal with in deepwater field developments (Kelland 2009). Compared to typical fluid hydrates with specific gravities of 0.8 or less, the gravity of the hydrate solid is typically 0.9 (E. Dendy Sloan 2003). This higher density leads to a problem of ensuring hydrate safety and preventing loss of property or lives (E. Dendy Sloan 2003).

There are various options to prevent hydrate crystallization. These options include heating, insulation, water removal and the use of chemical hydrate inhibitors (Kashchiev and Firoozabadi 2002). The most common chemical class for preventing gas hydrate formations is thermodynamic hydrate inhibitors, THIs (Sloan and Koh 2008), like methanol and glycols. The dosages of inhibitor needed, in wt% relative to water phase, are high (Kelland 2009). The development of alternative, cost-effective and environmentally acceptable gas hydrate inhibitors is a technical challenge for the oil and gas production industry (Kelland, Svartås et al. 1995). A new class of inhibitors, called low dosage hydrate inhibitors (LDHIs), has been established and is still under development (Oskarsson, Uneback et al. 2005).

The new class of hydrate inhibitors can lead to substantial cost savings, not only the reduced cost of the new inhibitor, but also for the size of the injection, pumping and storage facilities (Kelland, Svartås et al. 1995). The promise of LDHIs has been to provide a viable alternative to THIs such as methanol and glycol (Mehta, Hebert et al. 2002). These new chemicals are rapidly being adopted in the field and provide a fertile research era for molecular modeling (E. Dendy Sloan 2003).

While THIs are used in concentrations up to 60 wt%, the concentrations of LDHIs are typically 0.1-1.0 wt% based on the water phase (Kelland 2006).

Alcohols and glycols are THIs used to prevent gas hydrate formations (Sloan and Koh 2008). Methanol (CH_3OH) and monoethylene glycol, (MEG, $HOCH_2CH_2OH$) are widely used THIs used to protect against gas hydrate formation in production, workover, process operations and for melting hydrate plugs (Kelland 2009).

The focus in this report will be to study and establish an instrument for gas hydrate research. The instrument is a steel multi-cell rocker rig used to test one class of LDHIs called kinetic hydrate inhibitors (KHIs). The effectiveness and efficiency of KHIs are tested using the rocker rig, Rocking Cell RC5.

The measuring principle of the RC5 is based on a steady tilting of cooled, pressurized test cells. When the cells are tilting, a ball inside the chamber is rolling over the length of the test chamber mixing the fluid-gas mixture. Strong shear forces are created by the movement of the ball, and turbulence is created. In this way are the conditions in the pipelines reproduced in the test cells. The mixture inside the cells is distilled water and inhibitor, and an additional gas supply is used to achieve the right pressure conditions for the cells.

To establish the RC5 the main focus will be to study four already existing KHIs. The chemicals are Luvicap 55W, Luvicap EG, Inhibex 101 and Inhibex 501.

The chemicals is ranked according to how they work as hydrate inhibitors under pressure using two different cooling methods; a constant cooling method and an isothermal cooling method.

Luvicap 55W is used as a base chemical in order to see how the different parameters affect the gas hydrate formation. Parameters of interest are the rocking angle, the rocking speed, the cell volume, the type of ball used in the cells, the concentration and the cooling rate. The parameters are varied to see how they affect the results.

Chapter 2 gives a short introduction to gas hydrates, their composition and structure. The different classes of hydrate inhibitors are presented together with different test methods for LDHIs.

The relevant chemicals and the apparatus Rocking Cell RC5 are presented in Chapter 3, Materials and Methods. Standard parameters are introduced.

The results and discussion are found in Chapter 4, followed by a conclusion in Chapter 5.

2. Theory

2.1 Gas hydrates

The occurrence of gas hydrates in nature is controlled by an interrelation among the factors of temperature, pressure, and composition (Kvenvolden 1993). In the pressure-temperature domain of methane hydrates the position of the phase boundary is not only determined by the composition of the gas mixture, but also by the ionic impurities in the water (Kvenvolden 1993).

The first to report about natural gas hydrates was Sir Humphrey Davy in 1810, while the problem with hydrates in natural gas pipes was first documented by Hammerschmidt in 1934 (Sloan and Koh 2008). Since that the gas hydrate formation and dissociation phenomena have been the subject of numerous studies (Makogon 1997).

In nature very specific pressure conditions are required for gas hydrate stability. These conditions can be found in deep seabed deposits and permafrost, where the hydrates in addition may be preserved from dissociation by an ice layer (E. Dendy Sloan 2003). Gas hydrates are also common in aqueous chemical injection in gas lift lines if the pressure-temperature conditions are right (Kelland 2009). Gas hydrate stability in nature requires relatively high pressures, 100 – 300 bar, and low temperatures, from negative on the bottom of the sea up to 20 – 25 °C, though normally at temperatures lower than 15 – 20 °C (Makogon 1997).

Hydrates form at increasing pressures and at lower temperatures. It can be seen from Fig. 2-1 that the temperature below which hydrates can form increases with increasing pressure (Kelland 2009). A phase diagram for the CH_4-H_2O system is shown in Fig. 2-2, where clathrate dissociates to H_2O and CH_4 gas at low pressures or high temperatures (Stern, Kirdy et al. 1996).

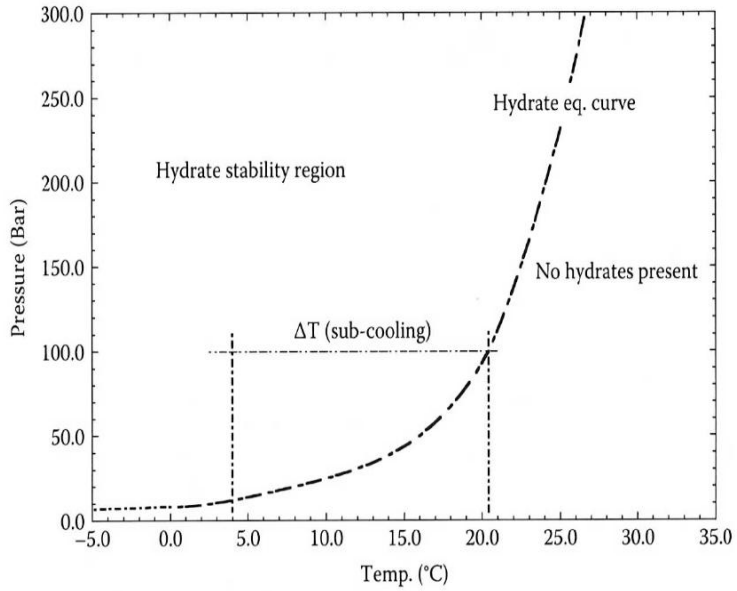

Fig. 2-1 Pressure-temperature graph for a typical natural gas hydrate (Kelland 2009).

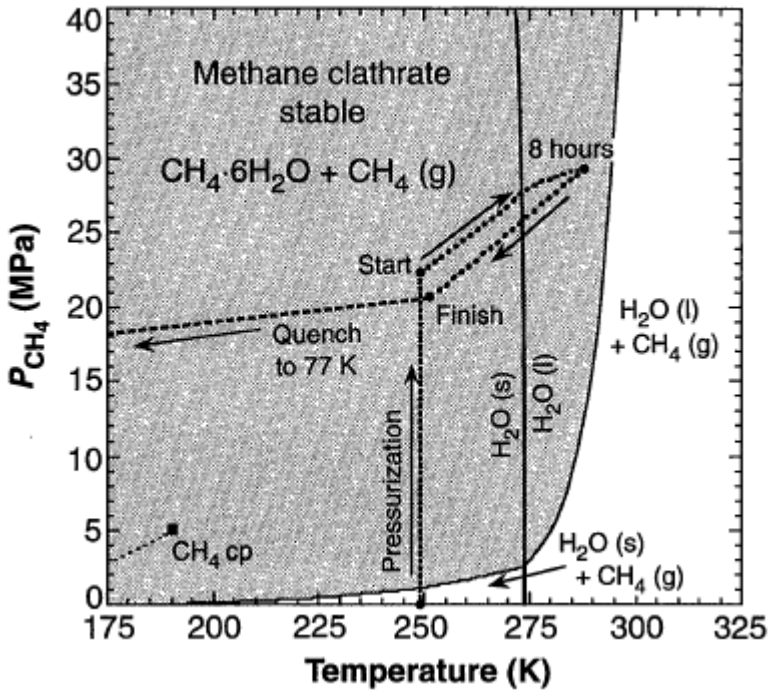

Fig. 2-2 Phase diagram for the CH_4-H_2O system. The field of methane clathrate stability is in the gray region. The metastable extension of the H_2O melting curve is delineated by the gray curve. Dotted lines trace the sample fabrication reaction path (Stern, Kirdy et al. 1996).

Methods to avoid hydrate plugs include raising the temperature by heating, lowering the pressure, removing the water and shifting the equilibrium for gas hydrate formations by adding anti-freeze chemicals (Kelland, Svartås et al. 2000).

2.1.1 Composition of gas hydrates

Natural gas hydrates are crystalline solids composed of water and gas (Sloan and Koh 2008), and are termed “clathrates” or inclusion compounds (Sloan 2011). Small paraffin guest molecules, like methane, ethane and propane, can be trapped in the network of cages of water molecules (Sloan 2011). Fig. 2-3 shows an example of a water molecule cage with a gas molecule occupied in it (Heroit-Watt-Institute-of-Petroleum-Engineering 2011). The hydrates are in many ways similar to ice formations, but can be formed at higher temperatures (Sloan and Koh 2008).

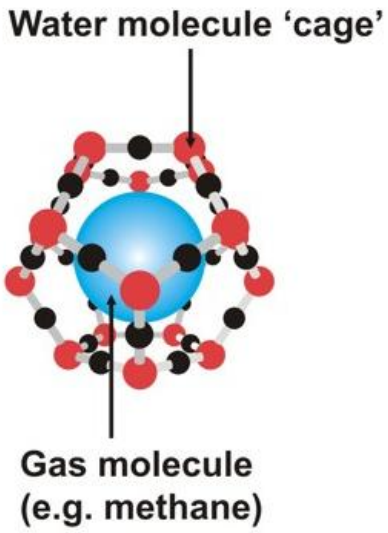

Fig. 2-3 A water molecule cage with gas molecule occupied in it. The figure is from (Heroit-Watt-Institute-of-Petroleum-Engineering 2011)

Hydrate nucleation is the process during which small clusters of water and gas grow and disperse in an attempt to achieve critical size for continued growth (Sloan and Koh 2008). The nucleation step is a microscopic phenomenon involving tens to thousands of molecules (Mullin 2001).

2.1.2 Gas hydrate formation and structure

In gas hydrates the water molecules form an open structure containing cages held together by hydrogen-bonding (Kelland 2009). These cages are occupied by small molecules, such as small hydrocarbons, which stabilize the clathrate structure through Van der Waals interactions (Kelland 2009) and capillary forces (Anklam, York et al. 2008).

There are three structures for gas hydrates to which all common natural gas hydrates belong. These are the cubic structure I, the cubic structure II and the hexagonal structure H, shown in Fig. 2-4 (Sloan and Koh 2008).

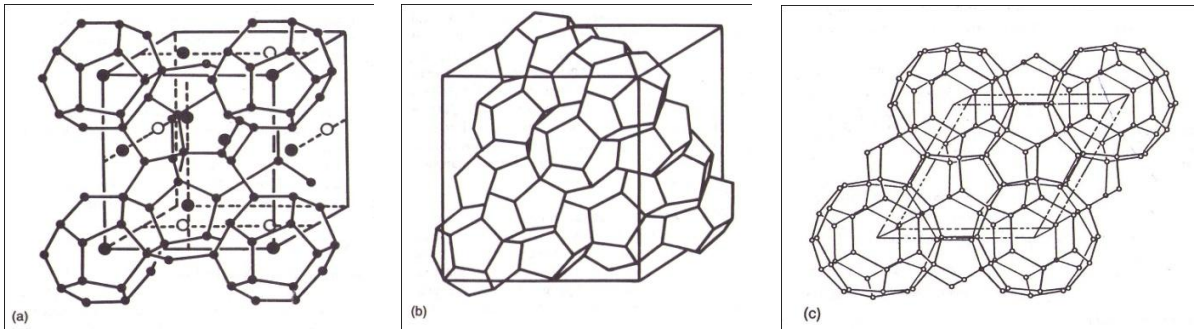

Fig. 2-4 The three gas hydrate formations; structure I, structure II and structure H as a), b) and c), respectively (Sloan and Koh 2008).

Structure I is mostly found in nature because methane is the major component in of most hydrates found outside the pipelines (Sloan 2011). These structures are formed with small molecules (smaller than 6 Å), like with methane, ethane, carbon dioxide and hydrogen sulfide (Sloan and Koh 2008).

Structure II hydrates occurs when somewhat larger molecules (6 Å < d < 7 Å) are present, for instance when the natural gas mixture include propane or iso-butane (Sloan and Koh 2008). The structure II hydrates are typically found in gas and oil operating processes (Sloan 2011), and is by far the most common hydrate structure found in the field, due to its stability whenever a natural gas mixture contains some propane or butane besides methane (Kelland 2009).

If even larger molecules (7 Å < d < 9 Å), such as iso-pentane or neohexane, are present in mixture with smaller molecules, like methane, hydrogen sulfide or nitrogen, structure H hydrates may form (Sloan and Koh 2008). This structure crystals are seldom found in artificial or in natural processes (Sloan 2011).

All three hydrate structures (I, II, and H) are approximately 85% (mol) water and 15% gas when all the cages are filled (Gabitto and Tsouris 2009). This fact suggests that the mechanical properties of the three hydrate structures are similar to those of ice (Gabitto and Tsouris 2009).

2.2 Gas Hydrate Inhibitors

There are generally two different classes of hydrate inhibition chemicals: (1) the traditional THIs, like methanol and monoethylene glycol, and (2) LDHIs, such as KHI and anti-agglomerants (AAs) (Sloan 2011). While the first class requires high concentrations of inhibitor to be successful is the latter one operated using low dosages of inhibitors/agglomerants (Kelland 2009).

The development of LDHIs started in the mid 1990s (Kelland 2006) and have been in commercial use in the upstream oil and gas industry for about 15 years (Kelland 2009). LDHIs are a cost-effective alternative to the traditional THIs (Lovell and Pakulski 2003). Neither of the two classes of LDHI will change the thermodynamic equilibrium of the hydrates, but rather change the hydrate kinetics and agglomeration, respectively (Kelland 2009). Both types are successfully used in fields applications (Kelland, Svartås et al. 2008). Economic drivers for further research on LDHIs are a wide range of OPEX savings, possible extended field lifetime and multi-million dollar CAPEX savings (Kelland 2006).

During deep-water oil and gas drilling, THIs are normally used while the KHIs and AAs are still under investigation (Ning, Zhang et al. 2010). The research on new LDHIs that can compete with the properties of the THIs is an ongoing process (Ning, Zhang et al. 2010). Extensive research has been conducted for the past few years in order to enhance the performance of LDHI and to improve the environmental profile (Fu, Housten et al. 2005).

2.2.1 Thermodynamic Hydrate Inhibitors

Thermodynamic hydrate inhibitors are the most common chemical class used to prevent gas hydrate formation. The objective of THIs is to maintain the pressures and temperatures of the flowline fluid (the black "S"-shaped line in Fig. 2-5) outside the gray hydrate region in Fig. 2-5 (Sloan 2011). To be effective for the flowline, the hydrate region should be displaced to the left, so that higher pressures or lower temperatures are required to form hydrates. In Fig. 2-5 about 23 wt% methanol is required in the free water in the flowline in order to keep the line outside of the gas hydrate formation region (Sloan 2011).

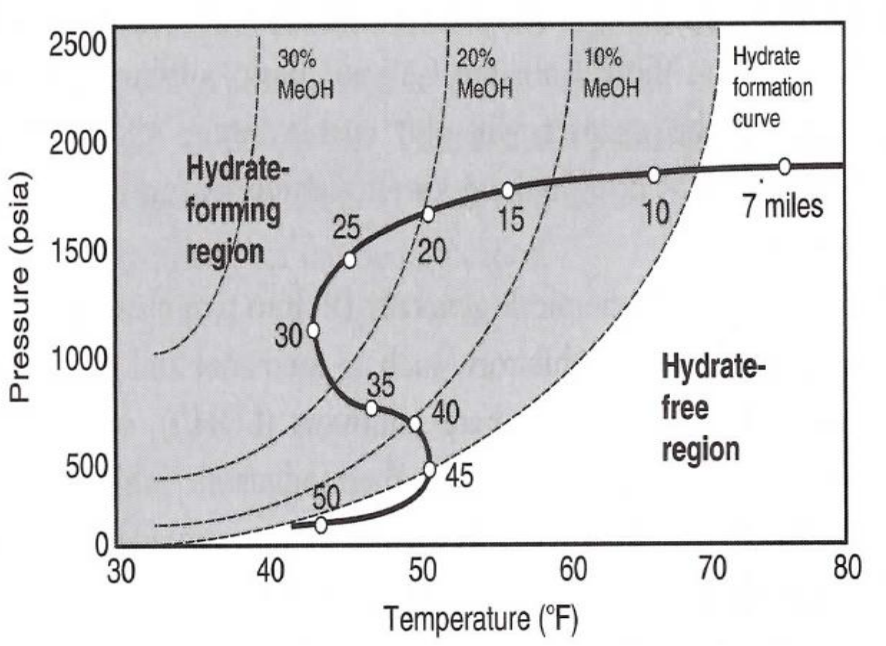

Fig. 2-5 Gas hydrate formation pressures and temperatures (gray region) as a function of methanol concentration in free water for a given gas mixture. Flowline fluid conditions are shown at distances along the bold black curve (Sloan 2011).

The addition of methanol and monoethylene glycol acts by preventing the water molecules from participating in the solid hydrate structure, but keeps them in the liquid flowable phase. The more inhibitor added to the system, the more water is prevented from participating in the hydrate structure, so higher pressures and lower temperatures, shown in Fig. 2-5, are required for gas hydrate formation from the remaining, uninhibited water (Sloan 2011).

By changing the bulk thermodynamic properties of the fluid system, the equilibrium conditions for gas hydrate formation are shifted to lower temperatures or higher pressures (Kelland 2009).

A big disadvantage with the THIs is the high concentrations needed, typically 20-60 wt% based on the water phase (Kelland 2006). The most common classes of THIs are alcohols, glycols and salts. Methanol and monoethylene glycol are two examples of respectively alcohol and glycols widely used (Kelland 2009). The correct dosing of THIs is very important since under-inhibition (when using a lower dose which won't totally protect against gas hydrate formation) can instead, at certain dosages, increase the plugging potential (Kelland 2009). Different calculation methods are used to find the correct amount of THI needed to avoid hydrate formation. They won't be discussed in this report.

Because of the high volume requirements of THIs, the costs for subsea multiphase transportation over long distances due to storage capacities, injection and regeneration facilities needed, are high (Kelland 2009). This was one of the starting points for research and development of a new class of hydrate inhibitors with the intention to find inhibitors that would achieve the same, or better, effect used at lower doses (Mehta, Hebert et al. 2002).

It has been reported that a mixture including methanol and a LDHI (Poly Vinyl Methyl Ester) was tested with real natural gas under gas hydrate formation conditions (Heidaryan, Salarabadi et al. 2010). The performance and efficiency of this combination turned out to be much better than using methanol alone. Advantages, such as significantly less volume injected, reduced freight costs, low toxicity, higher flash point and that the treatment was proven economical were found (Heidaryan, Salarabadi et al. 2010).

2.2.2 Kinetic Hydrate Inhibitors

The high costs of THIs have stimulated the search for KHIs (Lovell and Pakulski 2003).

KHIs are generally water-soluble polymeric compounds (Kelland 2006). Kinetic inhibition methods are based on injection of polymer-based chemicals at low dosage in the water phase (Fu 2002; Koh, Westacott et al. 2002). KHIs are delaying the initial hydrate nucleation, and have been used commercially in fields since around 1995 (Kelland 2009). KHIs make it possible for the produced fluid to be transported in a subsea multiphase from the field to the process facilities prior to the formation of hydrates in the pipes will start (Kelland 2009).

KHIs adsorb onto growing hydrate crystals at the hydrate/water interface and prevents the growth of hydrate crystals (E. Dendy Sloan 1997).

Typical concentrations that are used are less than 1 wt% of the water phase, usually around 0.3-0.5 wt% (Kelland 2009).

Since the first commercial use of KHI in Hyde/West Sole by BP in 1996, the number of KHI applications have grown exponentially over the last few years (Fu, Housten et al. 2005). The first generations of KHI are very effective in controlling hydrates up to 8°C subcooling and with extension of induction time to 24 hours (Fu, Housten et al. 2005). For the latest technology the application window was expanded to 13°C subcooling and for at least a 48-hour shut-in protection (Fu, Housten et al. 2005).

To test the performance of the KHIs, several methods are used. A common technique is by determine the minimum hold-time (the duration between the moment when the system enters the hydrate stability domain and the onset of gas hydrate formation) at the worst case subcooling field conditions (Klomp and Mehta 2007). Since the flowlines won't be at the maximum subcooling and pressure at all time, the result will give a conservative value of the dosage required to eliminate hydrate problems (Kelland 2009). For field verification under planned or unplanned shut-in conditions, shut-in tests with no flow have to be included. Experiments with the presence of other production chemicals (like corrosion inhibitors) should be run, since its known that many film-forming corrosion inhibitors may affect the performance of the KHIs negatively (Kelland 2009).

For optimal performances, the ideal molecular weight for a KHI polymer is usually around 1500-3000 (Del Villano 2009). If the molecular weight is below 1000 the performance of the KHI drops rapidly. At increasing molecular weights above 3000 the performance drops slowly, but does not disappear. A low molecular weight polymer has the added advantage of keeping the viscosity low, which is beneficial for the flow (Del Villano 2009).

KHIs work successfully by delaying the nucleation and growth of crystals, but fail to inhibit agglomeration of the crystals once nucleation starts (Oskarsson, Uneback et al. 2005). Due to this limitation the KHIs are less desirable for situations with long shut-in periods. But still, KHIs are used in low concentrations and are cost effective (Oskarsson, Uneback et al. 2005).

2.2.3 Anti-Agglomerants

AAs are surface active chemicals used in pipelines, not in drilling (Sloan and Koh 2008). As the name indicates, AAs prevent agglomeration. They do not attempt to prevent nucleation of hydrate crystals, rather they prevent the agglomeration and deposition of hydrate crystals and the consequent formation of plugs, such that a transportable hydrate slurry is formed (Kelland 2006). This class works better than KHIs when it comes to preventing gas hydrate formation plugging at higher subcooling. AAs are applicable for deepwater applications (Kelland 2009).

Two classes of AAs are commercially in use; production or pipeline AAs and gas well AAs (Kelland 2009). The first class allows the hydrates to form as transportable non-sticky slurry of hydrate particles dispersed in the liquid hydrocarbon phase. The second class, gas well AAs, disperse hydrate particles in an excess of water.

AAs require the presence of a liquid hydrocarbon phase to transport the suspension of the converted hydrate crystals. AAs cannot be used at high water cuts. (Kelland 2009).

2.3 Test apparatus for LDHIs

There are different types of equipment designed to study LDHIs. A very effective and simple technique to study growth inhibition involves measuring the growth rate of a single tetrahydrofuran, THF, hydrate crystal (Zeng, Wi et al. ; Makogon, Larsen et al. 1997). Threshold hydrate inhibitors form structure II hydrates, the same structure that is usually formed by natural gas hydrates.

Another apparatus is the ball-stop rig or rocker rig (Kelland 2006). The technique using rocking cells is based mainly on visual observation of a metal ball in motion (Oskarsson, Uneback et al. 2005). The ball moves back and forth in the cell, which rocks at a steady rate in a mixture of oil, water and gas under pressure and declining temperature. When formed, the hydrates can be seen through a sapphire window. If the formation of hydrates impacts the movement of the metal ball, it will be observed and usually considered catastrophic (Oskarsson, Uneback et al. 2005). When evaluating AAs, as in the case of hydrates where

they are allowed to form, they must be limited in size and spread to allow continuous movement of the ball (Oskarsson, Uneback et al. 2005). The rocking cells are in many cases used by service companies as the first step in qualifying a product (Kelland 2009). Both THF hydrate (Jussaume, Canselier et al. 1999; Talley, Mitchell et al. 2000) and natural gas hydrate (Deaton and Frost 1937; Talley, Mitchell et al. 2000) can be made in such ball-stop cells. The rocking rig using natural gas hydrate is a simple but excellent test equipment for AAs (Kelland 2006).

According to Klomp and Mehta (Klomp and Mehta 2007) Shell used rocking cells to assess the anti-hydrate activity of KHIs. The equipment is shown in Fig. 2-6.

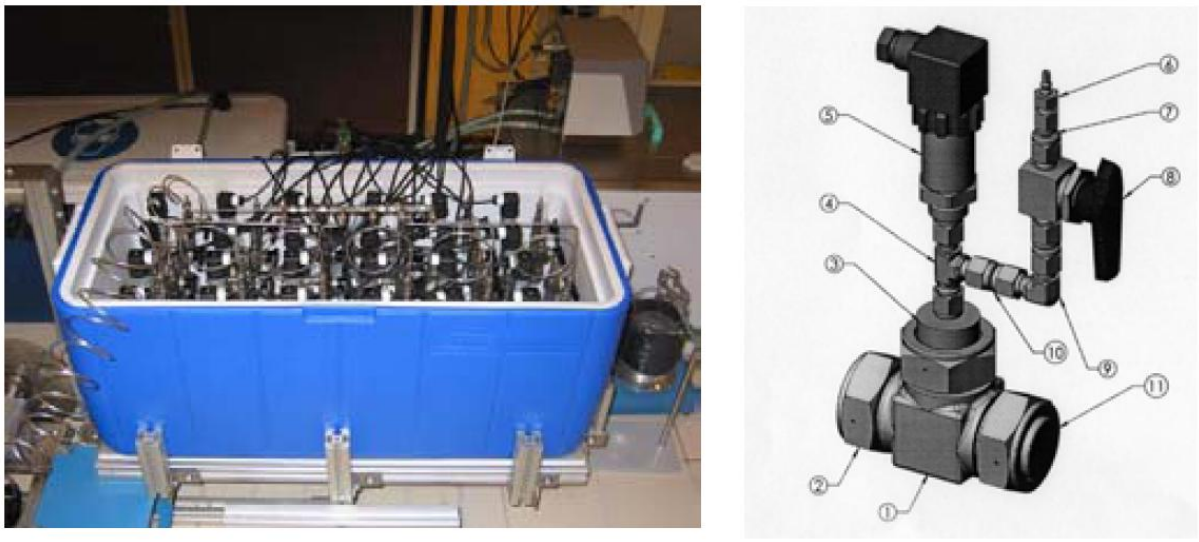

Fig. 2-6 The rocking cells used by Shell GSI. The picture to the left shows the whole cell assembly (containing 24 cells), as it is mounted to the seesaw. The figure to the right shows an individual cell and the main parts of which comprise: the 1'' tee (1), the end-nuts (2), the pressure transducer (5), a HP quick-connect gas inlet (6), a ball valve (8) and O-ring tightened blind flanges (11) (Klomp and Mehta 2007).

The University of Stavanger has recently invested in a Sapphire Rocking Cell (in co-operation with Statoil) to test LDHI. The sapphire test cells are entirely transparent and the whole sample chamber is visible for close observation of the samples behavior and the structure of the composed gas hydrates (PSL-Systemtechnik 2011). The measuring principle of the rocking cell is based on the constant rocking of temperature-controlled, pressurized test cells (PSL-Systemtechnik 2011). The technique using the sapphire rocking cells is based on the visual observation of a metal ball in motion, described earlier (Oskarsson, Uneback et al. 2005).

A high-pressure stirred cell or autoclave is also a commonly used apparatus (Arjmandi, Tohidi et al. 2005). An autoclave is an apparatus in which special conditions (high or low pressures or temperatures) can be established for a variety of applications, and make an ideal vessel for fast hydrate inhibitor hold-time determination (Sloan 2011). The cell is placed in a cooling bath where the pressure, temperature, and sometimes torque exerted on the stirrer are measured. Some cells have windows for visual observations while others are entirely made of sapphire (Kelland 2006). Mini-autoclaves have been developed for rapid screening of LDHIs (Lund, Akporiaye et al. 2004; Oskarsson, Lund et al. 2005; Oskarsson, Uneback et al. 2005).

Fig. 2-7 shows the set-up of a high pressure autoclave apparatus used to test KHI performances (Kelland 2006).

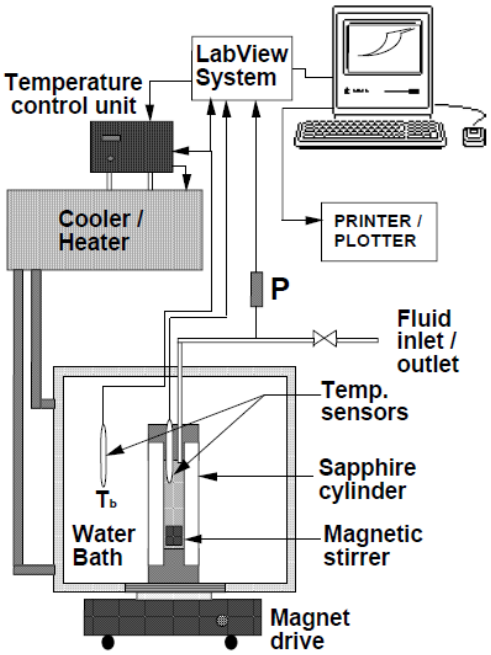

Fig. 2-7 Sapphire cell high pressure test equipment (Kelland, Svartås et al. 2000)

A more complex apparatus is the vertical placed pipe-wheel or loop-wheel. The pipe is usually of 1-3 inches in diameter, and can have a window for visual observation (Kelland 2006). It is pressurized before it's rotated in a cooling chamber (Kelland 2006). Pressure, temperature, and torque exerted on the wheel can be measured (Lippmann, Kessel et al. 1995; Urdahl, Lund et al. 1995; Lund, Urdahl et al. 1996). Tests in large loops and pipe wheels are generally the last and best step before the field trials or field implementation of the KHI (Kelland 2009).

Alternatively a horizontal flow loop can be used. A simple flow loop can used for tests using THF hydrates at atmospheric pressure, however, this type of loop has limited scope of use (Pakulski 1997). Most loops used today are high-pressure loops using natural gas, condensate, or oil and an aqueous phase (Kelland 2006). They can range from the mini-loop (e.g. ¼ inches in diameter) to the full scale pilot loop of 4 inches in diameter or more (Reed, Kelley et al. 1993; Talley, Mitchell et al. 2000).

3. Materials and methods

3.1 Solutions and chemicals

Four major KHIs are tested. Two are delivered by BASF Corporation and two from International Specialty Products, ISP. Luvicap 55W and Luvicap EG are both delivered by BASF, while Inhibex 101 and Inhibex 501 are delivered by ISP.

The first break-through in KHI technology came at CSM (Colorado School of Mines) in 1991, when they, during a ball-stop test, came across a polymer, poly(vinylpyrrolidone) (PVP), that delayed the formation and the agglomeration of THF hydrates, see Fig. 3- 1 (Long, Lederhos et al. 1994; Sloan 1995).

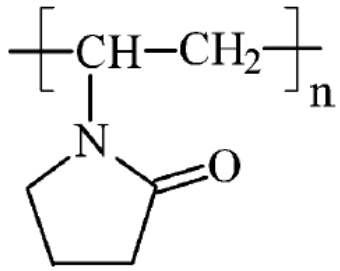

Fig. 3- 1 The structure of poly(vinylpyrrolidone).

PVP has five rings and is a member of the series of polyvinyllactams which have two main suppliers, BASF and ISP (Kelland 2006). CSM tested a hair-care product from ISP called Gaffix VC-713, a terpolymer, which contains a high proportion of the seven-ring monomer, vinylcaprolactam (VCap) as well as vinyl pyrrolidone (VP) and dimethylaminoethyl methacrylate (DMAEMA) (Kelland 2006). CSM also tested the homopolymer polyvinylcaprolactan (PVCap), see Fig. 3- 2 (Kelland 2006).

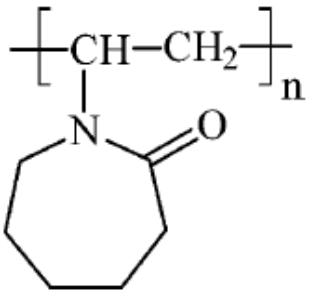

Fig. 3- 2 The structure of polyvinylcaprolactam (Kelland 2006).

It can be seen from Fig. 3- 3 that KHIs are polymers composed of polyethylene strands, from which are suspended lactam (with a N atom and a C=O group) chemical rings that are both approximately spherical in shape and polar (Sloan 2011). The key to the function of these KHI polymers is that they adsorb onto the surface of the hydrate, with the polymer pendant group as a "pseudo-guest", in a hydrate cage growing at the crystal surface (Sloan 2011).

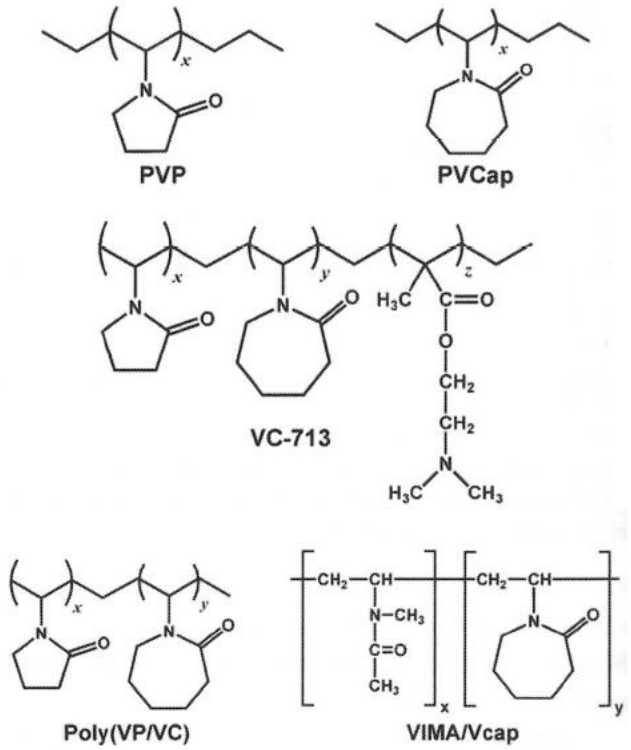

Fig. 3- 3 Repeating chemical formulas for four KHIs. Every line angle in the figure represents a CH_2 group. The upper horizontal angular line with a repeated parenthesis "( ) $_{x\ or\ y}$" in each structure suggests that the monomer structure is repeated "x or y" times to obtain a polymer (Sloan 2011).

The pendant lactam groups act to "anchor" the polyethylene polymer backbone to the $5^{12}6^4$ hydrate cages surface, and will not allow the polymer to dislodge (Sloan 2011). Two of the key KHI properties are (1) the pendant group on the polymer must fit into an incomplete, growing $5^{12}6^4$ cage; and (2) the spacing of the pendant groups on the polymer backbone must match the spacing of the growing $5^{12}6^4$ cages on the hydrate crystal surface, see Structure II in Fig. 3- 4 (Sloan 2011).

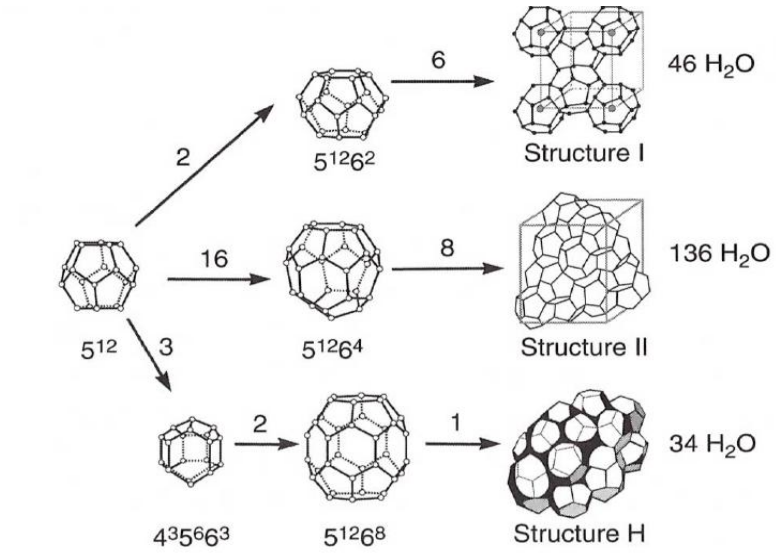

Fig. 3- 4 The three repeating hydrate unit crystals and their constitutive cages (Sloan 2011).

The concentrations of the four different gas hydrate inhibitors can be seen in Table 3- 1.

Table 3- 1 The concentrations of the relevant gas hydrate inhibitors.

Hydrate Inhibitor	Concentration
Luvicap 55W	53.8 wt% in water
Luvicap EG	41.1 wt% in monoethylene glycol (MEG)
Inhibex 101	50.0 wt% in butyl glycol ether (BGE)
Inhibex 501	50.0 Wt% in butyl glycol ether (BGE)

3.1.1 Composition of the Synthetic Natural Gas

The composition of the synthetic natural gas, SNG, used for the experiments is presented in Table 3- 2.

Table 3- 2 The composition of the SNG.

Component	Mole%
Methane	80.4
Ethane	10.3
Propane	5.0
Iso-butane	1.65
n-butane	0.72
N_2	0.11
CO_2	1.82

3.2 The Rocking Cell RC5

The test rig used for the experiments was delivered by PSL in the end of November 2010, and the first experiment was run the 1st of December. The rig is called Rocking Cell RC5, shortened RC5, and consists of 5 independent 40 ml rocker cells. Each of the cells has two magnets on the underside of them, used to fasten them on the contrary magnet in the cell bath.

Fig. 3- 5 shows the set-up of the rig. The set up includes the computer and the screen, the cooling bath placed under the computer, the vacuum pump on the left side of the computer and the RC5 Control Panel placed on top of the booster. A bottle of natural gas is connected to the RC5 control. The booster is used to reach the right pressure when the pressure in the natural gas bottle is below operational pressure.

The gas used for flushing the cells is transported through a pipeline out of the room and into a ventilation chamber. When flushing are the cells filled with 2-3 bar of nature gas and rocked for ca. 10 minutes. After rocking is the gas removed using a vacuum pump and released in the room. The amount of gas small and the emission is considered harmless.

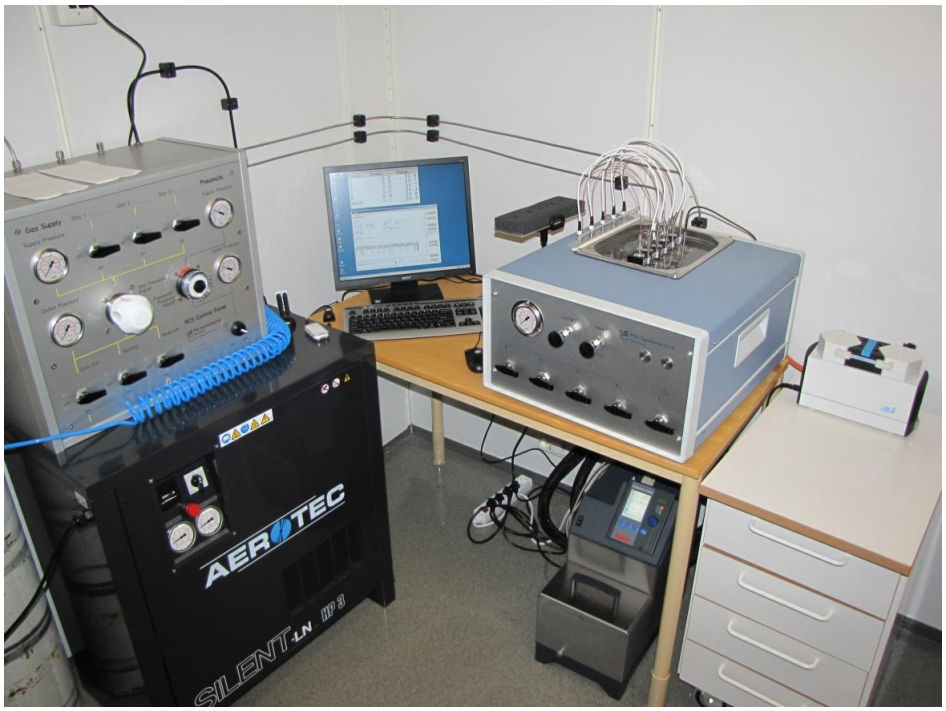

Fig. 3- 5 The complete set-up of the rig. The bottle with natural gas is barely visible in the left corner. The blue spiral pipe on top of the booster is a air gun used to dry the cells.

Fig. 3- 6 shows a picture of the cell bath and the 5 cells. The cells are connected to a temperature sensor, the white unit, and to a pressure sensor, the thin, orange unit. In the right corner of the bath is the cell bath temperature sensor.

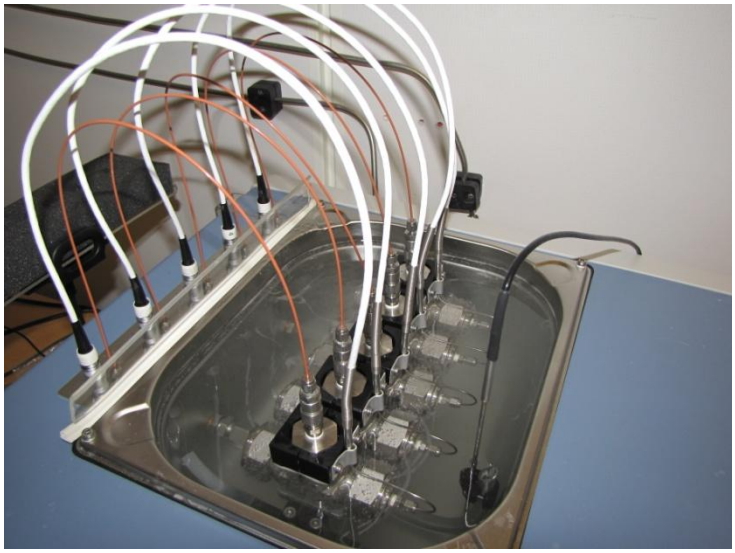

Fig. 3- 6 The 5 cells of the Rocking Cell 5.

A cooler device, the cooling bath, is located under the computer. Water circulates from the cooler to the cell bath and controls the temperature in the bath. The temperature can be

administrated either from the computer software WinRC or directly from the cooler, the Huber cryostat 230cc cooling bath.

There have been some problems with the temperature sensors as they have stopped working. They show no visible damage, but the temperatures they're logging are of big variation and log temperatures going from 16 °C to negative 30 °C in a matter of seconds. The consequences are not severe as there are 5 sensors and even if one is damaged there will still 4 sensors working.

New temperature sensor should be calibrated in accordance with the method described in the manual that followed the RC5.

From the start-up in December 2010 several new versions of the software have been uploaded on the customer page of PSL.

A big spanner is used to open and close the cover caps of the cells, see Fig. 3- 7. The cover should be tight, but not difficult to open. When placing the cells in the holder make sure that the temperature sensors won't have any sharp bends that may cause them damage.

Fig. 3- 7 The cover of the cells are fastened and loosened with a big spanner.

3.2.1 Test procedure

1) Starting the equipment

Make sure that the Huber cryostat 230cc cooling bath is started before turning on the computer using the button on the front of the RC5 – hold in for 3-4 seconds. This is to avoid problems controlling the temperature from the WinRC software.

2) Preparing the cells

The different cells should be placed on the same spot in the cell bath every time. The cells are marked from 1-5 on the temperature sensors. When the temperature sensors are changed, make sure to mark the new ones correctly. Use the same screw cap and ball for each of the cells.

a) For simplicity; start with cell 5. Place the ball in the cell and add wanted volume of solution. Some of the liquid may be lost due to splashing if the ball is added after the liquid.
   Be careful not to tilt the cell, as fluid may spill through gas inlet pipe.
b) When the cell is filled, fasten the cover cap using spanner, see Fig. 3- 7. The cap should be tight to avoid leakages.
c) Place the cell in the bath, and connect the temperature sensor (the white cable) and the gas cable (the orange cable).

Repeat this procedure for all the cells.

For safety reasons, place the plastic cover over the bath before flushing, rocking and pressurizing. The cover should be on until the experiment is finished.

3) Flushing

Flushing can be done in two ways:

i) Flushing the rocking cells 2 times at ca. 30 bar to remove air.
ii) Using a vacuum pump and pressurize with 2-3 bar of gas to remove air.

The second method, using a vacuum pump, is preferred in order to save gas.

i) Flushing using 30 bar pressure

On the "RC5 Control Panel":

a) Make sure that all valves are closed.
b) Open the gas bottle.
c) Open "Gas 1".
d) Open "Gas Out".

On the "Rocking Cell RC5":

a) Open the valves of the cells ready for flushing.
b) Close the "Inlet"/"Outlet" valve.
c) Close the valves of the cell.
d) Close "Gas Out"
e) Close the gas bottle.

Start rocking for 5-10 minutes. Be aware of potential leakages. This is seen as pressure drops higher than what is expected due to the temperature decrease. Use WinRC software to check the pressure.

Since this only takes 5-10 minutes can pkt. d) and e) above can be dropped. If the rocking goes on for a longer period pkt. d) and e) should be executed.

f) When the rocking is completed, stop the motor.
g) Start depressurizing the cells by opening the valves of the cells.

h) Depressurize slowly by opening the “Outlet” valve. Typical “outlet-speed” should not expand 1 bar per second. Some chemicals tend to start foaming, and high outlet-speed will increase the foam production.
i) When the (gauge) pressures in the cells are 0 bar: close the valves.

Repeat the procedure. When finishing pkt. i) the second time, start rocking again to see if the cell pressure increases. If there is any pressure left, open the cell valves and use the “Outlet” valve to release the pressure.

ii) Flushing using a vacuum pump

A safety device, a valve, is installed on the gas outlet pipe. The valve should point to the left (towards the screen) when the vacuum pump is not in use. As the valve points to the left, the gas (using the “Outlet” valve) is transported to the ventilation chamber.

When flushing the cells:

a) Make sure that the “Outlet” and “Inlet” valves are closed.
b) Turn the valve (found on the back of the computer) and make sure that the arrow points to the right (towards the vacuum pump).
c) Open the cells that should be flushed.
d) Turn on the vacuum pump.
e) Open the “Outlet” valve and let it pump for 5-10 minutes.

According to the instruction manual of the vacuum pump, 99% of the air is removed from the cells.

f) Close the “Outlet” valve.
g) Turn off the vacuum pump.
h) Fill the cells with 2-3 bar of natural gas, same procedure as for method i).
i) Close the cells and the “Inlet” valve and leave it rocking for 5-10 minutes.

The vacuum pump should be used again:

j) Open the cells.
k) Turn on the vacuum pump.
l) Open “Outlet” and leave it for 5-10 minutes.

The 2-3 bar of gas found in the cells will now be transported from the cells and out of the vacuum pump. The gas is released into the laboratory.

Another 99% of the air in the cells is removed, leaving a total of 0.01% air left in the cells.

m) Close the “Outlet” valve.
n) Turn off the pump.
o) Turn the valve (found on the back of the computer) 180^{o} so that the arrow points towards the screen.

The cells are ready to be pressurized.

4) Pressurizing

On the “RC5 Control Panel”:

If the pressure in the gas bottle is lower than operation pressure, boosting is necessary. This is explained in paragraph 5) Boosting.

Make sure all the valves are closed.

a) Open the gas bottle.
b) Open “Gas 1”.
c) Open “Gas Out”.

On the “Rocking Cell RC5”:

d) Open the valves ready for pressurizing.
e) Adjust the pressure with the “Inlet” and “Outlet” valves until wanted pressure is reached.

f) Close the “Inlet”/”Outlet” valve.
g) Close the valves of the cell.
h) Close “Gas Out”
i) Close the gas bottle.

5) Boosting

If the pressure in the gas bottle is lower than the operation pressure, boosting is necessary to reach the right pressure.

Make sure that the 5 cell valves are closed, as well as the outlet/inlet valves before starting the booster.

The booster is placed under the “RC5 Control Panel”, and has one on and off button, and a big, red emergency button.

a) As the booster is started, an increase in pressure can be seen on the Pneumatic pressure gauges on the “RC5 Control Panel”. When the pressure is sufficiently high, the booster should be turned off. The booster will stop automatically when the maximum pressure of 140 bar is reached.
b) Open the “Shift valve” on the “RC5 Control Panel” and boost as long as necessary. Close it as operation pressure is reached.
c) Open the cells before carefully opening the “Inlet” valve. Close when operation pressure is achieved.

If the pressure is still too low, repeat the process until sufficient pressure is achieved.
77 bar of pressure can be reached until there is ca. 8 bar left in the bottle.

6) Computer settings

The computer settings will vary depending on the type of experiment.

The settings in Table 3- 3 were used for the constant cooling method. The start temperature is 20.5°C. By choosing "Ramp" a stepwise decrease or increase in temperature is selected. In this case the temperature is said to decrease by 0.1°C every 6th minute. The time it takes to go from 20.5°C to 2.0°C which is the chosen temperature, is seen in the "Time" column. In this case, 18:30 (hh:mm).

2°C will be kept for 1 hour, before it is heated to 25°C in 1 hour. This is to make sure that all of the hydrates are melted. The temperature is kept at 25°C for 20 minutes. Finally the temperature is decreased to the start temperature, 20.5°C.

Table 3- 3 Computer settings used for the constant cooling method.

Step	Command	Rocking Rate	Angle	Set Temp [°C]	Time [hh:mm]	Ramp	Target Temp [°C]	Step Width [°C]	Step duration [m]
1	Flowing	20	40	20.5	18:30*	☑	2.0	0.1	6
2	Flowing	20	40	2.0	01:00	☐	-	-	-
3	Flowing	20	40	25.0	01:00	☐	-	-	-
4	Flowing	20	40	25.0	00:20	☐	-	-	-
5	Flowing	20	40	20.5	00:30	☐	-	-	-

* This value is based on step width and step duration.

Press "*Start Recording*".

The computer settings used for the isothermal method are shown in Table 3- 4. The rocking should start as wanted temperature is reached. The subcooling temperature is 7°C, and the start temperature is 20.5°C. If the temperature is reduced by 0.3°C every minute will the subcooling temperature be reached after 45 minutes. The rocking will start, and the cells are set to rock long enough for hydrate to form. The heating procedure is the same as for the constant cooling method.

Table 3- 4 Computer settings used for the isothermal method.

Step	Command	Rocking Rate	Angle	Set Temp [°C]	Time [hh:mm]	Ramp	Target Temp [°C]	Step Width [°C]	Step duration [m]
1	Flowing	1*	1*	20.5	00:45**	☑	7.0	0.3	1
2	Flowing	20	40	7.0	19:00	☐	-	-	-
3	Flowing	20	40	25.0	01:00	☐	-	-	-
4	Flowing	20	40	25.0	00:20	☐	-	-	-
5	Flowing	20	40	20.5	00:30	☐	-	-	-

* The lowest rate and angle possible.
** Depends on the width and step duration.

7) Depressurizing

On the "Rocking Cell RC5":

a) Open the cell valves.
b) Release pressure slowly (ca. 1 bar per second) until (gauge) pressure is 0, and rock for 5-10 minutes. If the pressure increases, open the relevant cells and release the pressure. The safety valve on the back of the computer should point towards the screen to avoid releasing the gas into the lab.

8) Cleaning the cells

Make sure there is no pressure in the cells as the cells are disconnected from the pressure sensors.

Note that the volume in the bath will decrease when the cells are removed. An alarm may go off on the Huber cryostat 230cc cooling bath. By closing the red pump valve on the cooling bath, the liquid will be kept in the cell bath. Distilled water can be added if the volume decreases. To restart the circulation, press start on the Huber menu → Scroll down to start circulation → Enter. Make sure to open the pump valve when the circulation is started.

a) For simplicity; start with cell 1.
b) Remove the screw cap and empty the cell.
c) Wash the cell, the ball and the screw cap according to this procedure:
    a. Zalo + water
    b. Tap water (make sure to remove ALL the Zalo from the equipment)
    c. Acetone
    d. Tap water
    e. Distilled water

A special sponge brush may be used if necessary.

d) Dry the equipment by using an air gun.
e) Place the cell, ball and screw cap in the special fitted suitcase. Make sure that the cells are placed on the right place; every cell has its own place, marked from 1-5.

Repeat this procedure for all 5 cells.

When not in use, the cells should be covered to protect them from the environment.

9) Updating the software

Software updates is found on the homepage of PSL Systemtechnik, http://www.psl-systemtechnik.de/haupt.html?&L=1. Username and passwords are found in the lab-book.

3.3 Cooling method

The performance of KHIs on gas hydrates can be tested using several methods, for instance:

A. An isothermal method (Cohen, Wolf et al. 1998; Sloan, Subramanian et al. 1998; Cingotti, Sinquin et al. 2000; Kelland, Svartås et al. 2000; Arjmandi, Tohidi et al. 2005; Lee and Englezos 2006; Del Villano, Kommedal et al. 2008).
B. A constant cooling method (Kelland, Svartås et al. 1994; Ajiro, Takemoto et al. 2010).
C. The ramping method (Reed, Kelley et al. 1993; Colle, Oelfk et al. 1999; Del Villano, Kommedal et al. 2009).

The methods used in this report is method A (isothermal) and B (constant cooling), and these are presented in Chapter 3.3.1 and 3.3.2. Method C is not used in this report, but is briefly mentioned in Chapter 3.3.3.

3.3.1 Constant cooling method

When using a constant cooling method the computer settings are similar to what is found in Table 3- 3 in the test procedure in section 3.2.1. The cells are filled with distilled water and inhibitor and cooled down to a very low temperature (high subcooling) (Del Villano and Kelland 2011). For the experiments in this report the water and the inhibitor was cooled down to 2°C. Typical results of pressure, temperature and time can be seen in Fig. 3- 8.

The cooling is carried out in a closed vessel over a short period of time, and the induction time, t_i, is difficult to determine since the pressure also drops due to the cooling of the fluid (Del Villano and Kelland 2011). The induction time in gas hydrate crystallization is an important characteristic of the kinetics of the process. Long induction time would allow transport of fluids through the production facilities to the processing plant without crystallization of hydrates in the system (Kashchiev and Firoozabadi 2002). The induction time, also called the nucleation delay time, is dependent on the subcooling in the system – higher subcooling gives a lower induction time (Del Villano and Kelland 2011).

In Fig. 3- 8 the lines on the bottom represents the data of the temperature sensors. The temperature can be read on the vertical axis to the right. The lines on the top show the data of the pressure sensors. The pressure slowly starts to decrease after ca. 900 minutes. At this point the pressure is ca. 69 bar and the temperature is ca. 7°C. After ca. 1000 minutes a fast pressure drop can be seen, at a pressure of ca. 66 bar and temperatures around 4°C.

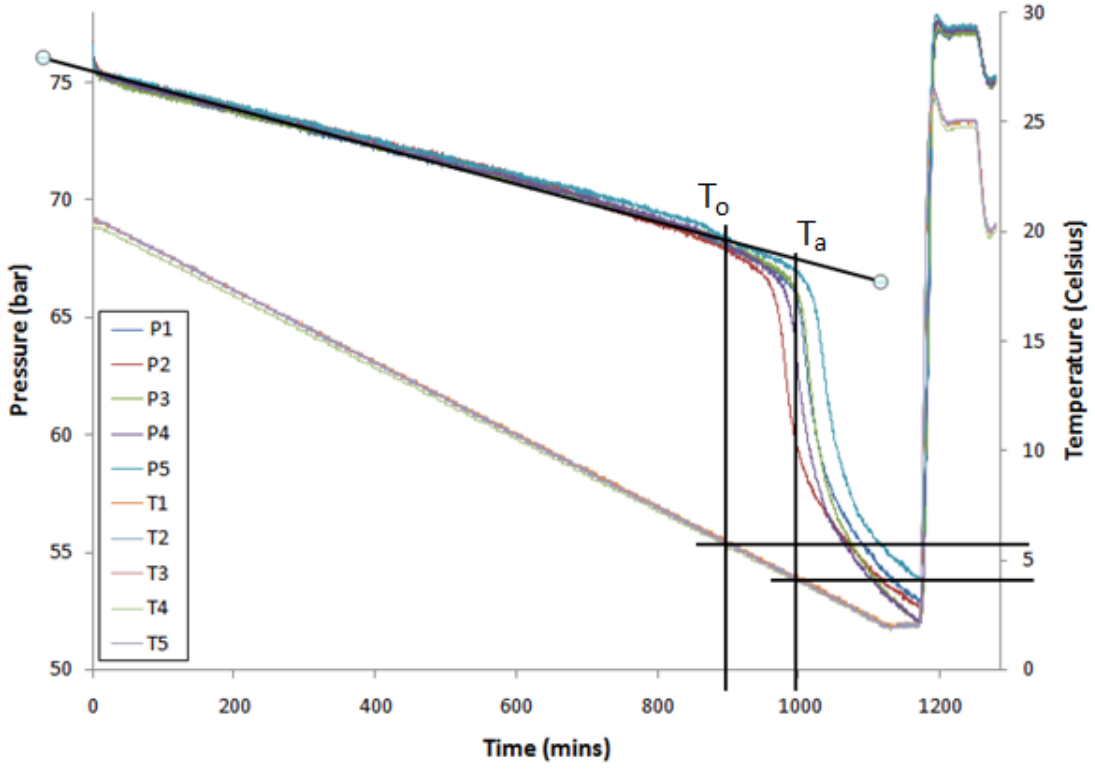

Fig. 3- 8 Testing Luvicap 55W at 5000 ppm 03.12.10.

3.3.2. Isothermal method

The isothermal method is based on cooling the fluids in the cells to a certain subcooling without rocking. The computer settings are similar to what is presented in Table 3- 4 in section 3.2.1. The cells will start rocking as the temperature is reached. The first sign of pressure drop is called the induction time, t_i. Hydrates may have formed earlier than this, but they are not detected. The time between the t_i and t_a (rapid gas hydrate formation, see Chapter 3.3.5) is the period in which the hydrate crystals are growing slowly, and the pressure is

slowly decreasing. The rapid growth of gas hydrates can be seen as a strong decrease in pressure (Del Villano and Kelland 2011), see Fig. 3- 9.

In Fig. 3- 9 the lines on the bottom represents the temperature sensors. The temperature can be read from the vertical axis to the right. From the readings it's visible that the rocking temperature is 6°C and it is reached after ca. 60 minutes, t_i. The lines on the top are the data from the pressure sensors. Ca 400 minutes after 6°C was reached (t_o-t_i, in this case: 460 mins – 60 mins) the pressure slowly starts to decrease. At this point the pressure is ca. 68 bar. 460 minutes after 6°C was reached (t_a-t_i, in this case: 520 mins – 60 mins) a rapid pressure drop is observed. The pressure is ca. 64 bar.

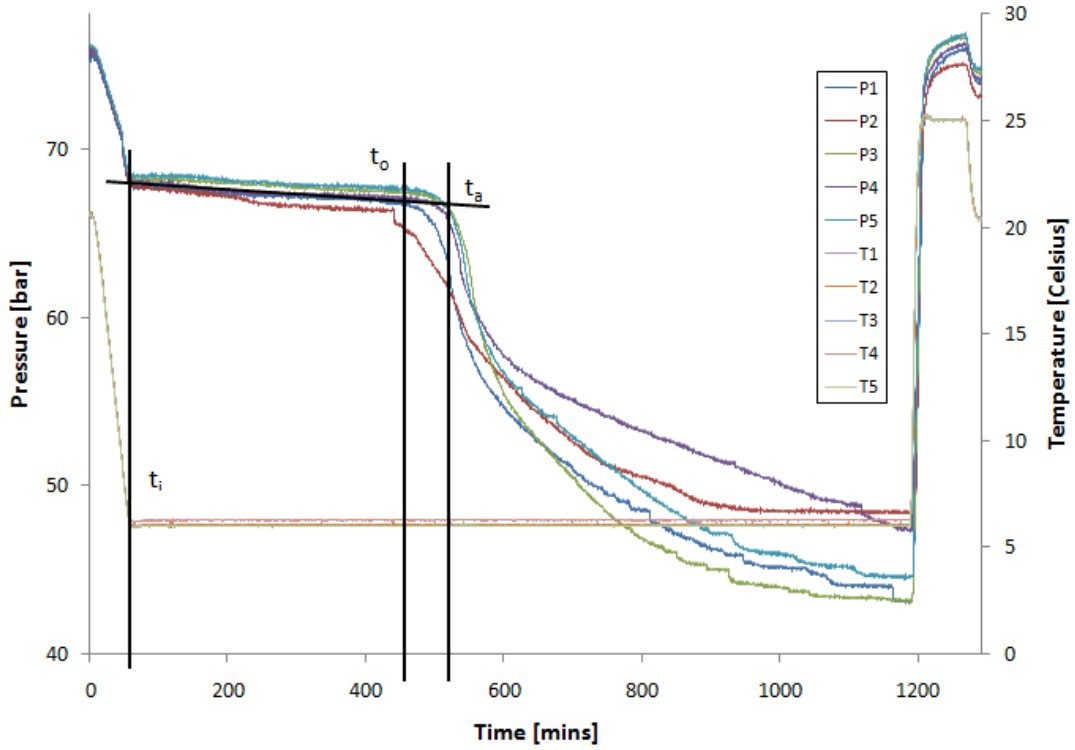

Fig. 3- 9 Testing Luvicap 55W at 5000 ppm 18.03.11.

3.3.3 Ramping method

This method is carried out by stepwise cooling. The fluids are cooled (with agitation) to a certain subcooling, held at this temperatures for typically a few hours, then cooled rapidly to a higher subcooling and then held again (Del Villano and Kelland 2011). This is repeated

several times until hydrates have formed. As mentioned earlier in the report this method was not used, but a typical graph of a ramping KHI test can be seen in Fig. 3- 10 (Del Villano and Kelland 2011).

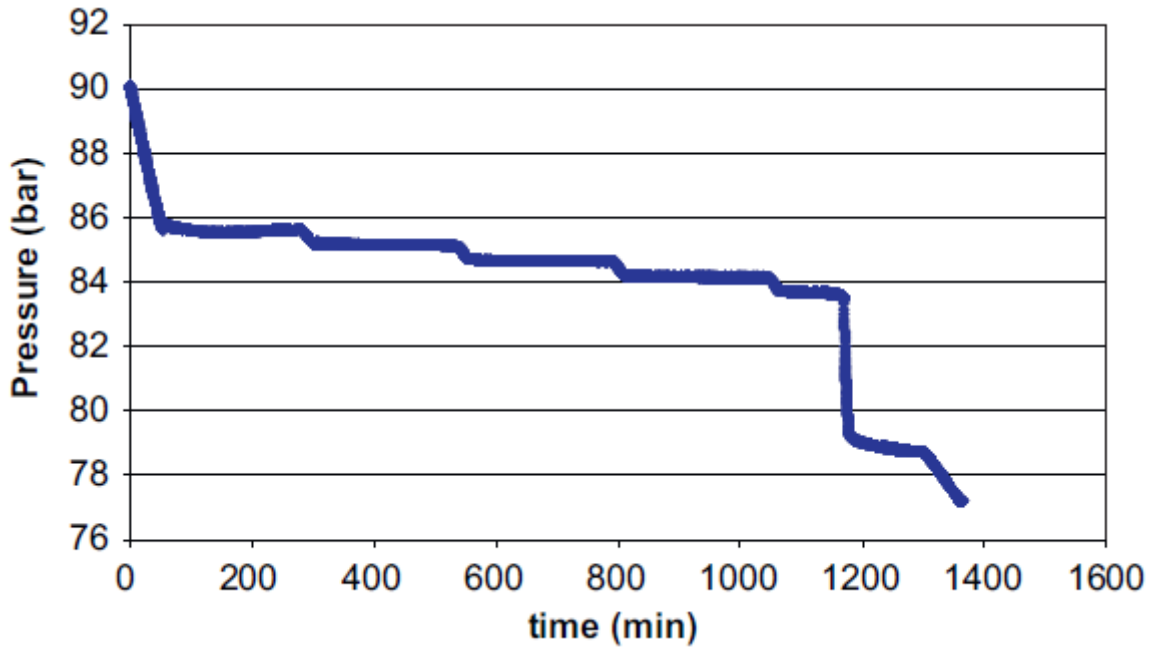

Fig. 3- 10 A ramping test of a KHI in a closed vessel. Rapid gas hydrate formation can be seen at 1180 min after the start of the experiment (Del Villano and Kelland 2011).

3.4 Gas hydrate onset temperature

The gas hydrate onset temperature, T_o, is defined as the temperature of a system being cooled at which hydrates are first detected (Sloan 2011). Invisible hydrate nucleation and crystal growth events actually takes place before a system reaches T_o. This is found where the linear pressure line starts to deviate from its path. This exact point may be difficult to spot, but by drawing a linear line following the pressure and see where the pressure line is deviating from the drawn line, T_o can be found, see Fig. 3- 11.

In Fig. 3- 11 a linear line is drawn following the pressure drop. At 6.3°C the pressure line clearly starts to deviate from the drawn line, and gas hydrates have started to form.

The gas hydrate onset temperature is named T_o [°C] for constant cooling method and t_o [mins] for the isothermal method for the rest of the report.

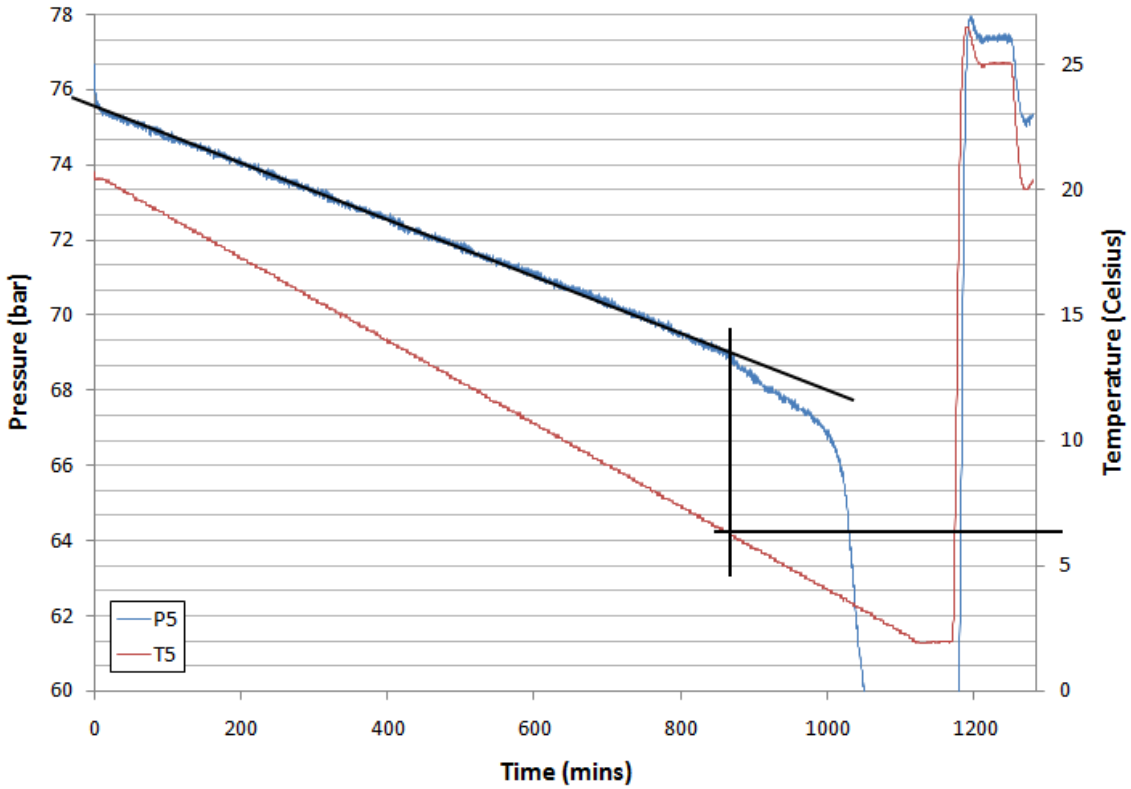

Fig. 3- 11 Luvicap 55W 5000 ppm tested 03.12.10, cell number 5.

3.5 Rapid gas hydrate formation temperature

After the first gas hydrates starts to form there is a snow ball effect and at a certain point the formation will reach its maximum. This point when the gas hydrate formation is most rapid is called the point of rapid gas hydrates formation. From the graph this point is found where the slope is the steepest, see Fig. 3- 12.

In Fig. 3- 12 a vertical line is drawn from the steepest point at the pressure line until it crosses the temperature line. In this case the rapid gas hydrate formation temperature is at 3.8°C.

The rapid gas hydrate formation temperature is named T_a [°C] for constant cooling method and t_a [mins] for the isothermal method for the rest of the report.

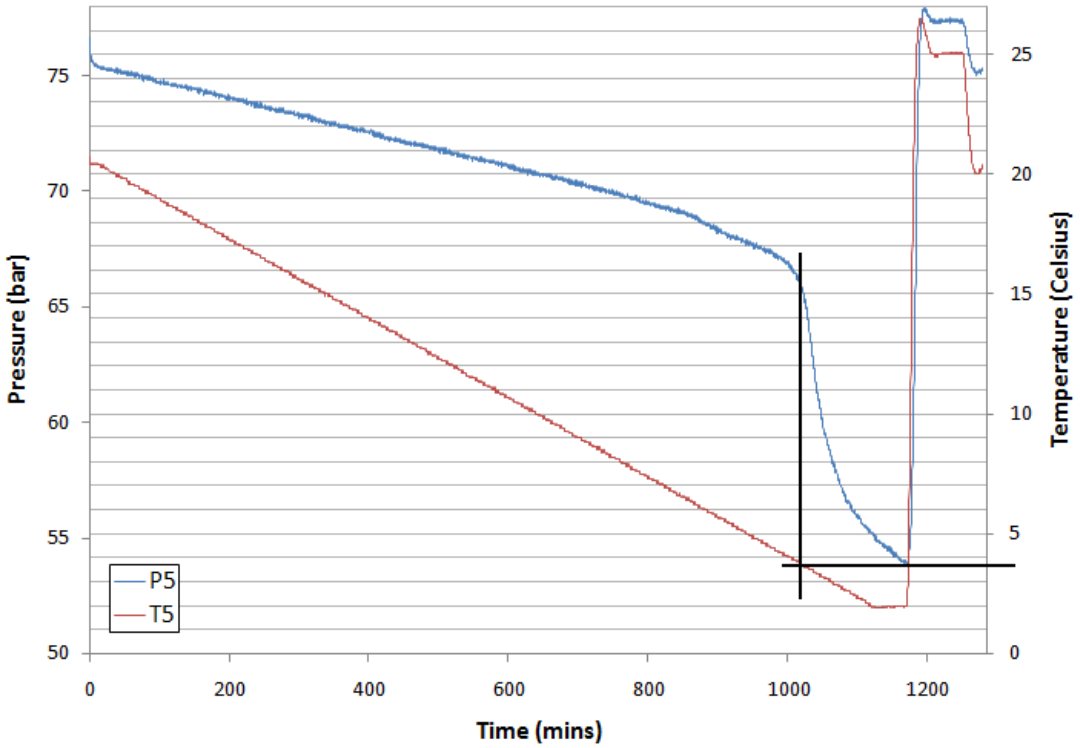

Fig. 3- 12 Luvicap 55W 5000 ppm tested 03.12.10, cell number 5.

3.6 Isobaric operation

The start pressure is ~76 barg (77 bar) for all the experiments, and no pressure is released during the test. The first pressure drop is due to decreasing temperature. In isobaric operation the system pressure is maintained constant, by the exchange of gas or liquid with an external reservoir (Sloan and Koh 2008). The temperature is decreased until the formation of hydrate is indicated by significant addition of gas (or liquid) from a reservoir (Sloan and Koh 2008). After gas hydrate formation the temperature is slowly increased (maintaining constant pressure by fluid withdrawal) until the last crystal of hydrate disappears (Sloan and Koh 2008). This point, taken as the equilibrium temperature of gas hydrate formation at constant pressure, may be determined by visual observation of hydrate dissociation or at a constant temperature as simple hydrate dissociate with heat input (Sloan and Koh 2008).

3.7 Delta pressure

In the Appendix [A] Table of Results is a column reporting the pressure drop for each cell, due to gas hydrate formation. This value is not exact, but it still gives an estimate on what the pressure drop caused by the hydrates will be.

The pressure drop is found by subtracting the pressure before hydrates started to form from the pressure after hydrates have formed, and before the temperature starts increasing (from 2°C), see Fig. 3- 13. For simplicity are the pressure before hydrates start to form said to be around 66 bar for all the experiments. The delta pressure, DP, for Fig. 3- 13 is therefore 12 bar (66 bar – 54 bar).

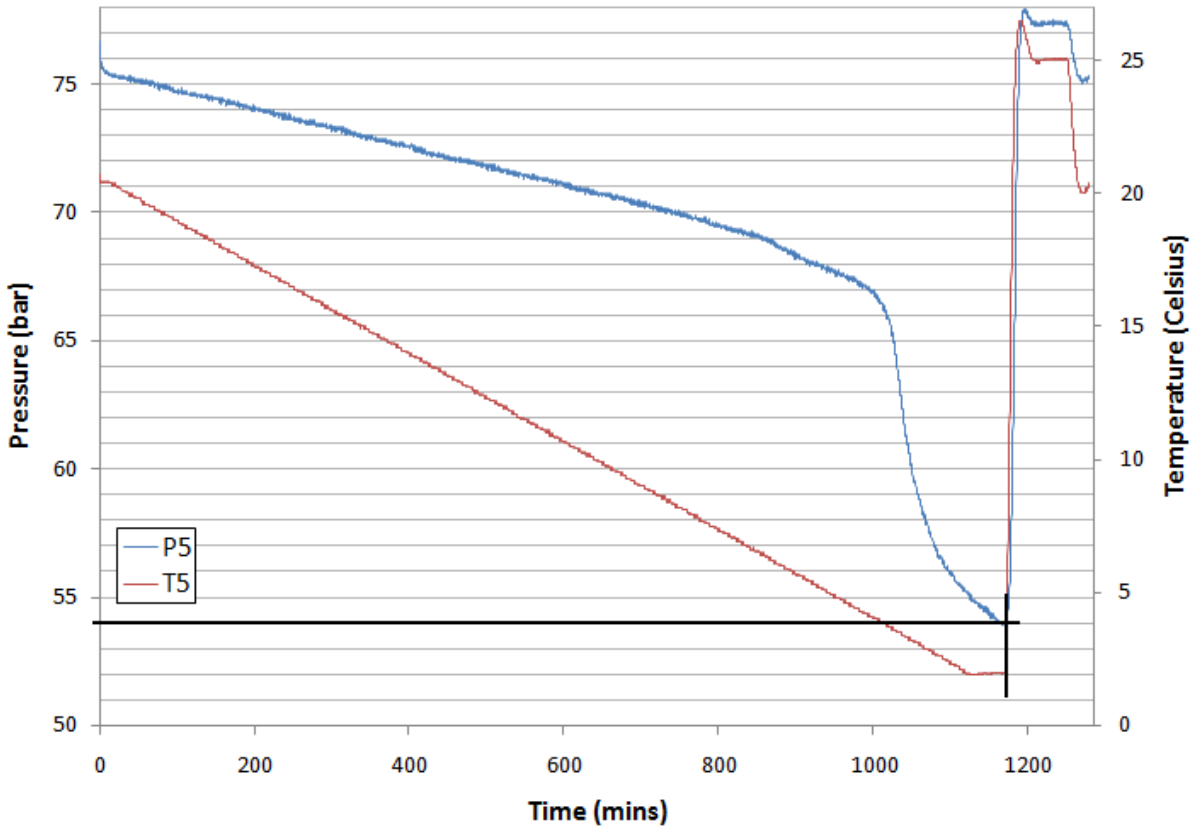

Fig. 3- 13 Luvicap 55W 5000 ppm tested 03.12.10.

3.8 Parameters

Some parameters are changed in order see how they'll impact the gas hydrate formations.

3.8.1 Standard parameters

Some standard conditions are set in order to get comparable results from the experiments. The standard parameters are shown in Table 3- 5.

Table 3- 5 Standard parameters used for testing gas hydrate formations at the RC5.

Parameter	Value
Cell volume	20 ml
Rocking rate	40 rocks per minute
Rocking angle	40°
Rocking ball	Steel ball
Concentration	2500 ppm and 5000 ppm

For the isothermal method experiments the standard subcooling temperature is set to 7°C.

3.8.2 Changes in the parameters

In order to see how the different parameters would affect the gas hydrate formation, the parameters were changed, one at the time.

- The cell volume was increased from 20 ml to 30 ml in each cell, and decreased from 20 ml in each cell to 10 ml.
- The rocking rate was reduced from 20 rocks per minute to 10 rocks per minute.
- The rocking angle was reduced from 40° to 25°.
- The steel balls were replaced with glass balls with a rougher surface.

- The concentration was also tested at 1000 ppm and at 10 000 ppm.

- The cooling rate was tested at “fast”, where cooling process took ca. 6 hours, at “normal” where the cooling process lasted for ca. 18 hours, and “slow” where the cooling process took ca. 54 hours.

The results from these changes can be seen in Chapter 4 Results and Discussion.

4. Results and Discussion

The experiments were set to start rocking at 7°C using the isothermal method.

KHI performance tests were carried out in a high pressure rocker rig, and initial pressure was ca. 77 bar. Standard natural gas was used for all the experiments. Structure II hydrates were formed. For all the experiments the aqueous phase was distilled water.

The calculations of percentage deviation can be seen in Appendix [C] Calculations.

4.1 How changing the aqueous liquid volume in the cells affects the results

The cell volume was decreased from standard 20 ml to 10 ml in each cell, and increased from standard 20 ml in each cell to 30 ml in each cell. Using the constant cooling method the experiments were run at concentrations of 2500 ppm and 5000 ppm, while only 5000 ppm was tested using the isothermal method.

Constant cooling method

Results show that an increase in cell volume lead to a decrease in T_o and T_a values. This can be seen graphically in Fig. 4-1 (2500 ppm), and in Fig. 4-2 (5000 ppm), and in numbers in Table 4-1 (2500 ppm) and Table 4-2 (5000 ppm).

At 2500 ppm the average T_o values were:

At 10 ml : 8.3°C
At 20 ml : 7.1°C
At 30 ml : 6.4°C

At 2500 ppm the average T_a values were:

At 10 ml : 6.7°C
At 20 ml : 5.8°C
At 30 ml : 5.0°C

When the volume was reduced from 20 ml in each cell to 10 ml, the average T_o value increased with 16.9%. The corresponding average T_a value increased with 15.5%.

When the volume was increased from 20 ml in each cell to 30 ml, the average T_o value decreased with 9.9%. The corresponding average T_a value decreased with 13.8%.

Table 4-1 Data used to make Fig. 4-1. The content of the cells is Luvicap 55W and distilled water at a concentration of 2500 ppm. The tests were performed 08.03.11 (10 ml), 27.01.11 (20 ml) and 10.03.11 (30 ml). The data is extracted from Appendix [A] Table of Results.

Volume [ml]	T_o [°C]	T_a [°C]
10	8.0	6.3
10	8.3	6.8
10	8.2	6.7
10	8.6	6.9
10	8.2	6.8
20	7.0	5.9
20	7.0	5.8
20	7.1	5.8
20	7.4	5.8
30	6.3	5.0
30	6.8	5.0
30	6.4	5.0
30	6.4	5.0
30	6.3	5.0

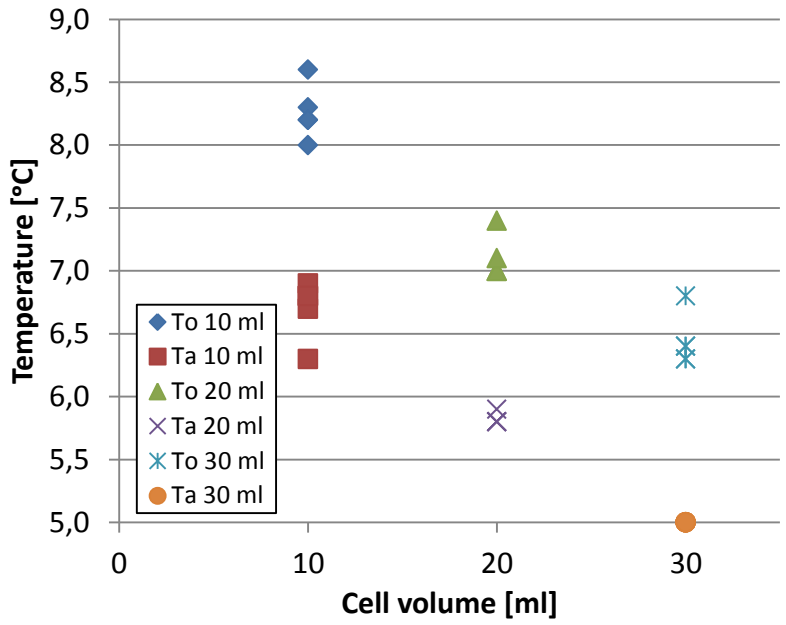

Fig. 4-1 The relationship between T_o and T_a values and different cell volumes, using Luvicap 55W at 2500 ppm. The highest temperatures at each volume are from 2500 ppm.

At 5000 ppm the average T_o values were:

At 10 ml : 6.3°C
At 20 ml : 6.2°C
At 30 ml : 4.8°C

At 5000 ppm the average T_a values were:

At 10 ml : 4.3°C
At 20 ml : 3.4°C
At 30 ml : 2.2°C

When the volume was reduced from 20 ml in each cell to 10 ml, no statistically significant difference was observed on the average T_o. The corresponding average T_a value increased with 26.5%.

When the volume was increased from 20 ml in each cell to 30 ml, the average T_o value decreased with 22.6%. The corresponding average T_a value decreased with 35.3%.

Table 4-2 Data used to make Fig. 4-2. The content of the cells are Luvicap 55W and distilled water at a concentration of 5000 ppm. The tests were performed 09.03.11 (10 ml), 02.02.11 (20 ml) and 14.03.11 (30 ml). The data is extracted from Appendix [A] Table of Results.

Volume [ml]	T_o [°C]	T_a [°C]
10	6.9	4.3
10	6.4	4.2
10	6.0	4.1
10	5.9	4.2
10	6.4	4.8
20	6.3	3.5
20	6.2	3.3
20	6.1	3.5
20	6.1	3.5
20	6.5	3.4
30	4.4	2.2
30	4.9	2.3
30	4.9	2.0
30	4.8	2.3
30	5.1	2.0

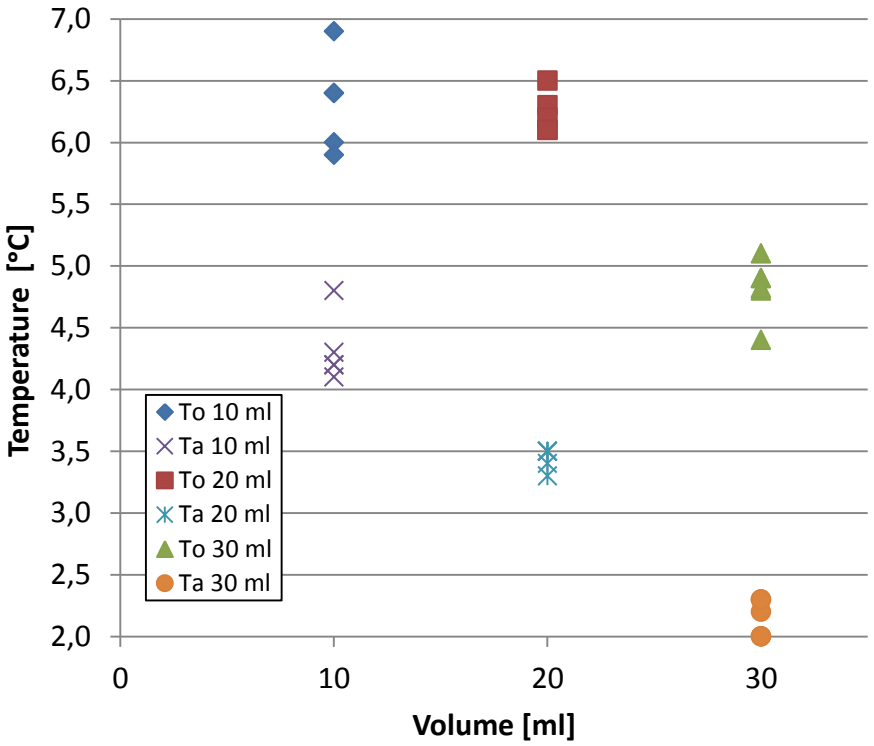

Fig. 4-2 The relationship between T_o and T_a values and different cell volumes, using Luvicap 55W at 5000 ppm. The highest temperatures at each volume are from 2500 ppm.

Isothermal method

Results show that an increase in cell volume lead to an increase in t_o and t_a values. This can be seen graphically in Fig. 4-3, and in numbers in Table 4-3.

At 30 ml the experiment was stopped after 1132 minutes as no gas hydrates were formed.

At 5000 ppm the average t_o values were:

At 10 ml : 211 mins
At 20 ml : 650 mins
At 30 ml : >1132 mins

At 5000 ppm the average t_a values were:

At 10 ml : 243 mins
At 20 ml : 699 mins
At 30 ml : >1132 mins

When the volume was reduced from 20 ml in each cell to 10 ml, the average t_o value decreased with 67.6%. The corresponding average t_a value decreased with 65.2%.

When the volume was increased from 20 ml in each cell to 30 ml, the average T_o value increased with > 74.2%. The corresponding average t_a value increased with > 61.9%.

Table 4-3 Data used to make Fig. 4-3 and Fig. 4-4. The content of the cells are Luvicap 55W and distilled water at a concentration of 5000 ppm. The experiments were performed 04.04.11 (10 ml), 28.03.11 (20 ml) and 03.04.11 (30 ml). The data is extracted from Appendix [A] Table of Results.

Volume [ml]	t_o [mins]	t_a [mins]
10	197	213
10	226	238
10	141	-
10	281	294
10	208	226
20	504	542
20	657	718
20	677	721
20	871	932
20	543	582
30	>1132	>1132
30	>1132	>1132
30	>1132	>1132
30	>1132	>1132
30	>1132	>1132

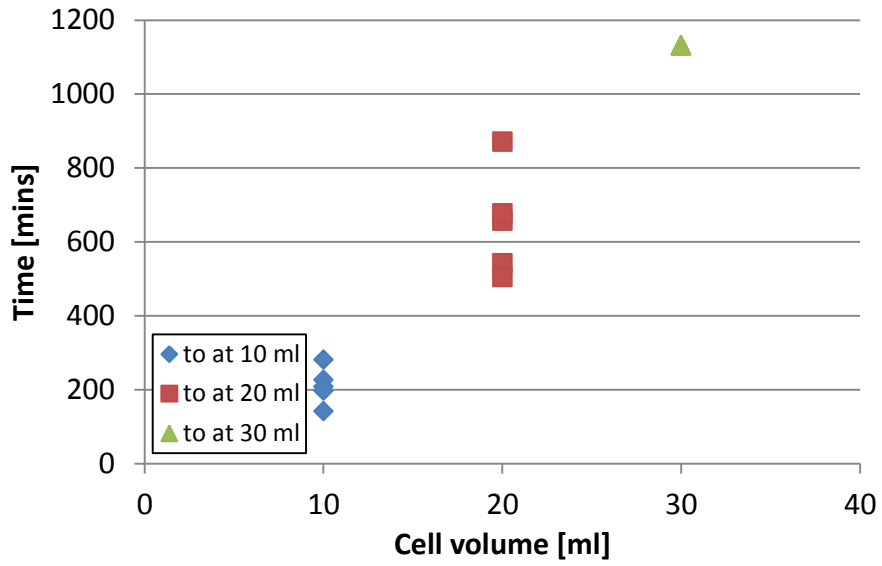

Fig. 4-3 The relationship between t_o and t_a values and different cell volumes, using Luvicap 55W at 5000 ppm.

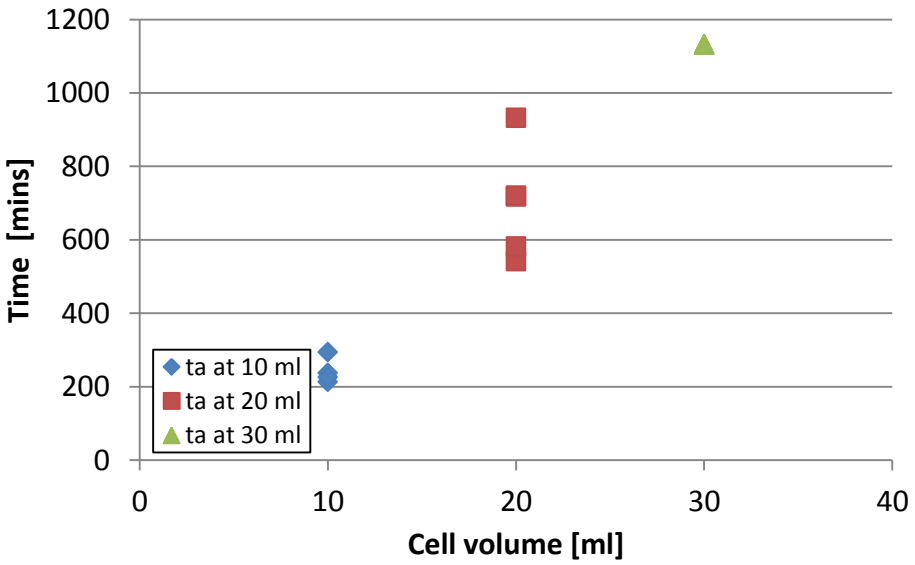

Fig. 4-4 The relationship between t_o and t_a values and different cell volumes, using Luvicap 55W at 5000 ppm

Comments:

Though the equilibrium temperature remains the same for all the experiments, the result show that the induction time increased as the volume increased.

One explanation may be that when going from 10 ml water to 30 ml of water, one may go from a gas excess system to a water excess system. This may affect the PVT response, but most likely not the "true growth".

More water means more inhibitor and more hydrates can be formed by a smaller gas volume and at a correspondingly greater pressure drop in the cells. From Appendix [A] Table of Results, the pressure drop in the cells (due to gas hydrate formations) increased with increased cell volume:

10 ml in each cell gives a pressure drop of (2500 ppm/5000 ppm) : 3.2/2.5 bar
20 ml in each cell gives a pressure drop of (2500 ppm/5000 ppm) : 10.3/9.8 bar
30 ml in each cell gives a pressure drop of (2500 ppm/5000 ppm) : 36.5/26.3 bar

The gas – water ratio could affect contact surface between these phases in some way that affect the probability of nucleation.

4.2 How changing the rocking rate affects the results

The rocking rate was decreased from standard 20 rocks per minute to 10 rocks per minute. Using the constant cooling method the experiments was run at concentrations of 2500 ppm and 5000 ppm, while only 5000 ppm was tested using the isothermal method.

Constant cooling method

Results at 2500 ppm show that a decrease of the rocking rate lead to an increase in average T_o, while average T_a was the same at both rates. This can be seen graphically in Fig. 4-5, and in numbers in Table 4-4.

Results at 5000 ppm show that a decrease of the rocking rate lead to a decrease in average T_o and a small increase in average T_a value. This can be seen graphically in Fig. 4-6, and in numbers in Table 4-5.

At 2500 ppm the average T_o values were:

At 10 rocks per minute : 8.1°C
At 20 rocks per minute : 7.1°C

At 2500 ppm the average T_a values were:

At 10 rocks per minute : 5.8°C
At 20 rocks per minute : 5.8°C

When the rocking rate was reduced from 20 rocks per minute to 10 rocks per minute, the average T_o value increased with 14.1%.

Table 4-4 Data used to make Fig. 4-5. The content of the cells are Luvicap 55W and distilled water at a concentration of 2500 ppm. The experiments were performed 23.02.11 (10 rocks per minute) and 27.01.11 (20 rocks per minute). The data is extracted from Appendix [A] Table of Results.

Rocking rate [rocks per minute]	T_o [°C]	T_a [°C]
10	8.2	5.9
10	8.2	5.8
10	8.7	5.8
10	8.1	5.7
10	7.2	6.0
20	7.0	5.9
20	7.0	5.8
20	7.1	5.8
20	7.4	5.8

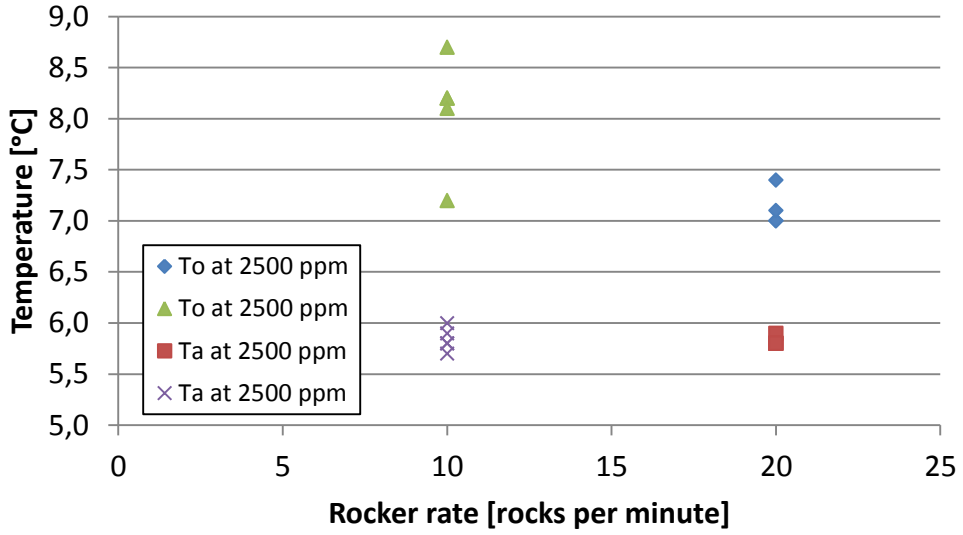

Fig. 4-5 The relationship between T_o and T_a values and different rocking rates, using Luvicap 55W at 2500 ppm.

At 5000 ppm the average T_o values were:

At 10 rocks per minute : 5.6°C
At 20 rocks per minute : 6.6°C

At 5000 ppm the average T_a values were:

At 10 rocks per minute : 3.7°C
At 20 rocks per minute : 3.5°C

When the rocking rate was reduced from 20 rocks per minute to 10 rocks per minute, the average T_o value decreased with 15.2%. The corresponding average T_a increased with 5.7%.

Table 4-5 Data used to make Fig. 4-6. The content of the cells are Luvicap 55W and distilled water at a concentration of 5000 ppm. The experiments were performed 21.02.11 (10 rocks per minute) and 02.02.11 (20 rocks per minute). The data is extracted from Appendix [A] Table of Results.

Rocking rate [rocks per minute]	T_o [°C]	T_a [°C]
10	5.3	3.7
10	5.9	3.4
10	5.7	3.6
10	5.3	3.8
10	5.8	3.8
20	6.8	3.5
20	6.8	3.5
20	6.8	3.5
20	6.2	3.3
20	6.2	3.7

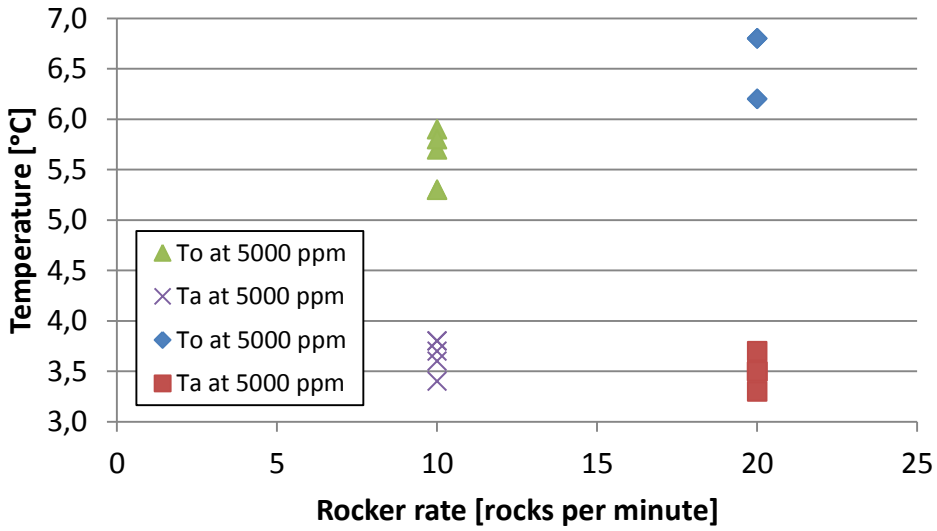

Fig. 4-6 The relationship between T_o and T_a values and different rocking rates, using Luvicap 55W at 5000 ppm.

Isothermal method

Results show that a decrease in rocking rate leads to a decrease in t_o and t_a values. This can be seen graphically in Fig. 4-7 (t_o) and Fig. 4-8 (t_a), and in numbers in Table 4-6.

At 5000 ppm the average t_o values were:

At 10 rocks per minute : 589 mins
At 20 rocks per minute : 650 mins

At 5000 ppm the average t_a values were:

At 10 rocks per minute : 660 mins
At 20 rocks per minute : 699 mins

When the rocking rate was reduced from 20 rocks per minute to 10 rocks per minute, the average t_o value decreased with 9.4%. The corresponding average t_a value decreased with 5.6%.

Table 4-6 Data used to make Fig. 4-7 and Fig. 4-8. The content of the cells are Luvicap 55W and distilled water at a concentration of 5000 ppm. The experiments were performed 29.03.11 (10 rocks per minute), 28.03.11 (20 rocks per minute). The data is extracted from Appendix [A] Table of Results.

Rocking rate [rocks per minute]	t_o [mins]	t_a [mins]
10	630	704
10	648	721
10	479	548
10	586	652
10	600	674
20	504	542
20	657	718
20	677	721
20	871	932
20	642	582

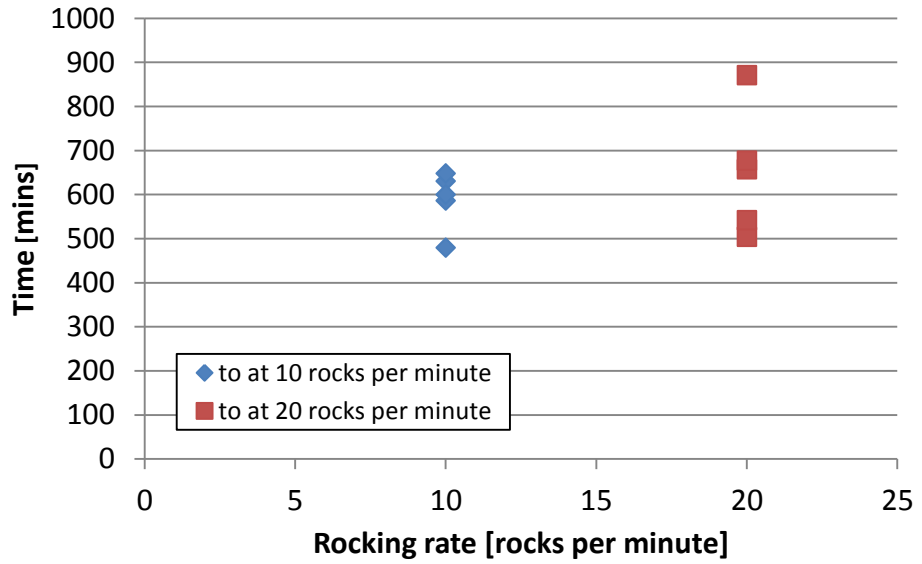

Fig. 4-7 The relationship between t_o values and different rocking rates, using Luvicap 55W at 5000 ppm.

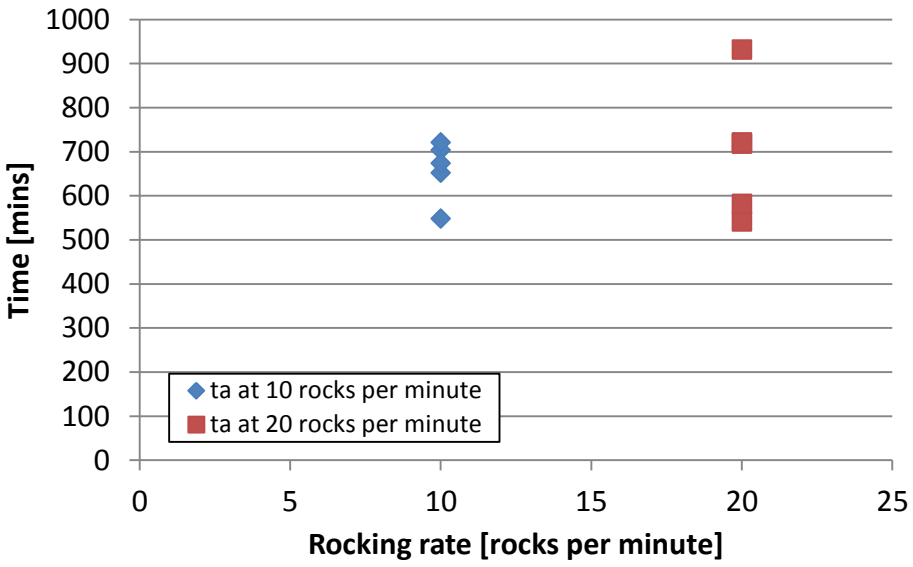

Fig. 4-8 The relationship between t_a values and different rocking rates, using Luvicap 55W at 5000 ppm.

Comments:

At 5000 ppm (constant cooling method) the reduction of the rocking rate improves the performance of the hydrate inhibitor, while at 2500 ppm (constant cooling method) the performance of the hydrate inhibitor decreased as the rocking rate is reduced. For the isothermal experiment the performance of the hydrate inhibitor decrease as the rocking rate is reduced.

Anklam (et al.) writes that if particles are held together by dispersion forces alone, and if the particles are separated by a steric barrier of a few nanometers, then shear forces under typical flow conditions should be sufficient to break apart flocks to particles (Anklam, York et al. 2008). Reducing the rocking rate may give weaker shear forces and flocks won't be broken apart. Though reducing the rocking rate of the cells in the RC5 might not affect the shear rates enough to see a change the induction time/temperature.

More experiments should be performed to get a better answer on how the rocking rate affects the inhibition of gas hydrates.

4.3 How changing the rocking angle affects the results

The rocking angle was decreased from standard 40° to 25°. Using the constant cooling method the experiments were run at concentrations of 2500 ppm and 5000 ppm, while only 5000 ppm was tested using the isothermal method.

Constant cooling method

Results at 2500 ppm show that a decrease of rocking angle just lead to a small increase in average T_o while the average T_a was the same at both concentrations. This can be seen graphically in Fig. 4-9, and in numbers in Table 4-7.

Results at 5000 ppm show that a decrease of rocking angle lead to a decrease in average T_o while the average T_a was the same for both angles. This can be seen graphically in Fig. 4-10 and in numbers in Table 4-8.

At 2500 ppm the average T_o values were:

At 25° : 7.4°C
At 40° : 7.1°C

At 2500 ppm the average T_a values were:

At 25° : 5.8°C
At 40° : 5.8°C

When the rocking angle was reduced from 40° to 25° no statistically significant difference was observed, neither for average T_o nor average T_a.

Table 4-7 Data used to make Fig. 4-9. The content of the cells are Luvicap 55W and distilled water at a concentration of 2500 ppm. The experiments were performed 02.03.11 (25°) and 27.01.11 (40°). The data is extracted from Appendix [A] Table of Results.

Rocking angle [°]	T_o [°C]	T_a [°C]
25	7.4	5.5
25	8.0	6.0
25	7.8	5.8
25	6.9	5.9
25	7.0	5.7
40	7.0	5.9
40	7.0	5.8
40	7.1	5.8
40	7.2	5.8

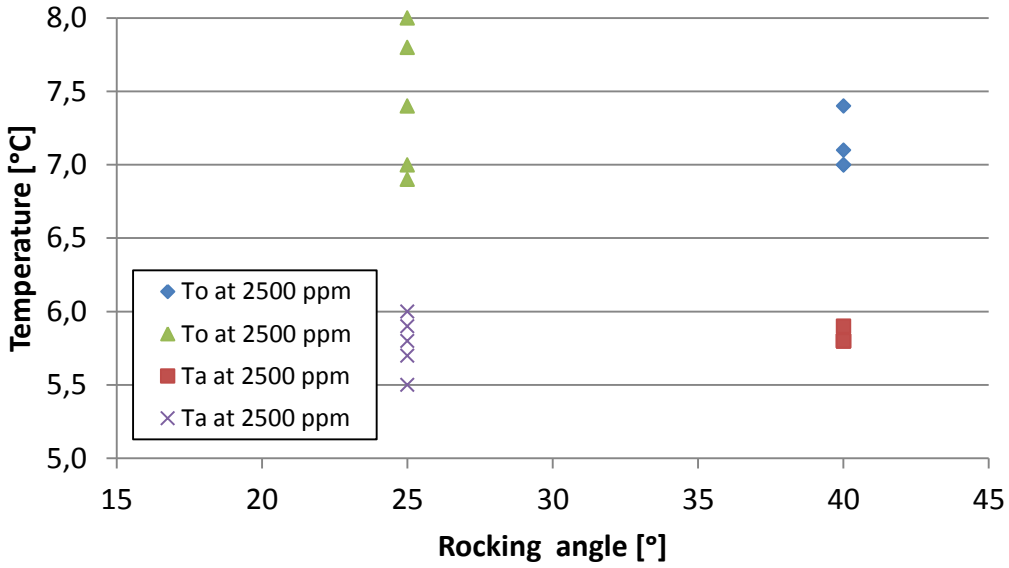

Fig. 4-9 The relationship between T_o and T_a values and different rocking angles, using Luvicap 55W at 2500 ppm.

At 5000 ppm the average T_o values were:

At 25° : 6.2°C
At 40° : 6.6°C

At 5000 ppm the average T_a values were:

At 25° : 3.5°C
At 40° : 3.6°C

When the rocking angle was reduced from 40° to 25°, the average T_o value decreased with 6.1%. No statistically significant difference was observed for average T_a.

Table 4-8 Data used to make Fig. 4-10. The content of the cells are Luvicap 55W and distilled water at a concentration of 5000 ppm. The experiments were performed 03.03.11 (25°) and 02.02.11 (40°). The data is extracted from Appendix [A] Table of Results.

Rocking angle [°]	T_o [°C]	T_a [°C]
25	6.9	3.9
25	5.8	3.4
25	6.0	3.4
25	6.1	3.6
25	6.3	3.6
40	6.8	3.5
40	6.8	3.5
40	6.8	3.5
40	6.2	3.3
40	6.2	3.7

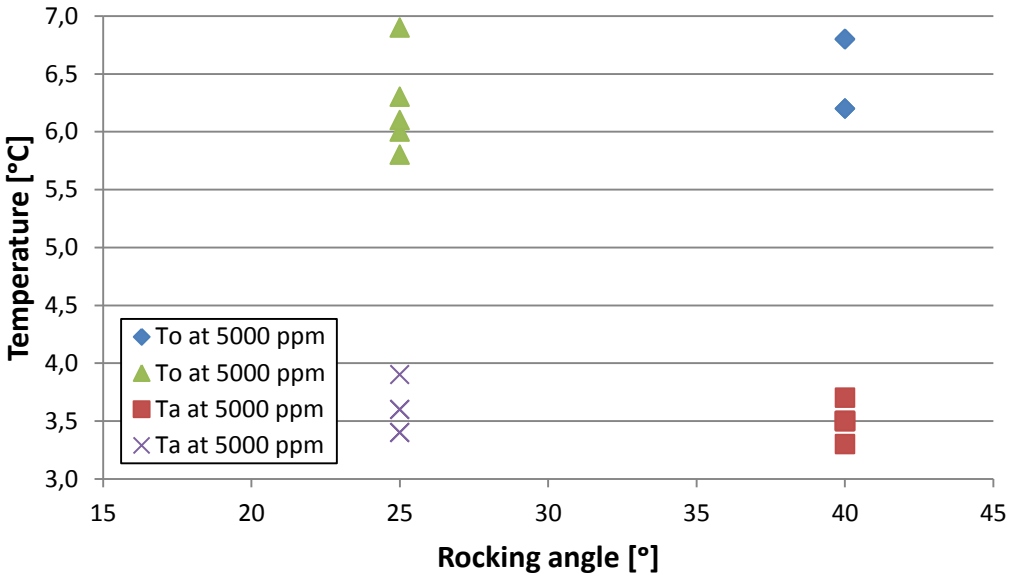

Fig. 4-10 The relationship between T_o and T_a values and different rocking angles, using Luvicap 55W at 5000 ppm.

Isothermal method

Results show that a decrease in rocking angle leads to an increase in t_o and t_a values. This can be seen graphically Fig. 4-11 (t_o) and Fig. 4-12 (t_a), and in numbers in Table 4-9.

At 5000 ppm the average t_o values were:

At 25° : 654 mins
At 40° : 650 mins

At 5000 ppm the average t_a values were:

At 25° : 723 mins
At 40° : 699 mins

When the rocking angle was reduced from 40° to 25°, no statistically significant difference was observed, neither for average t_o nor average t_a.

Table 4-9 Data used to make Fig. 4-11 and Fig. 4-12. The content of the cells are Luvicap 55W and distilled water at a concentration of 5000 ppm. The experiments were performed 02.04.11 (25°) and 28.03.11 (40°). The data is extracted from Appendix [A] Table of Results.

Rocking angle [°]	t_o [mins]	t_a [mins]
25	703	733
25	643	719
25	697	768
25	679	749
25	546	606
40	504	642
40	657	718
40	677	721
40	871	932
40	542	582

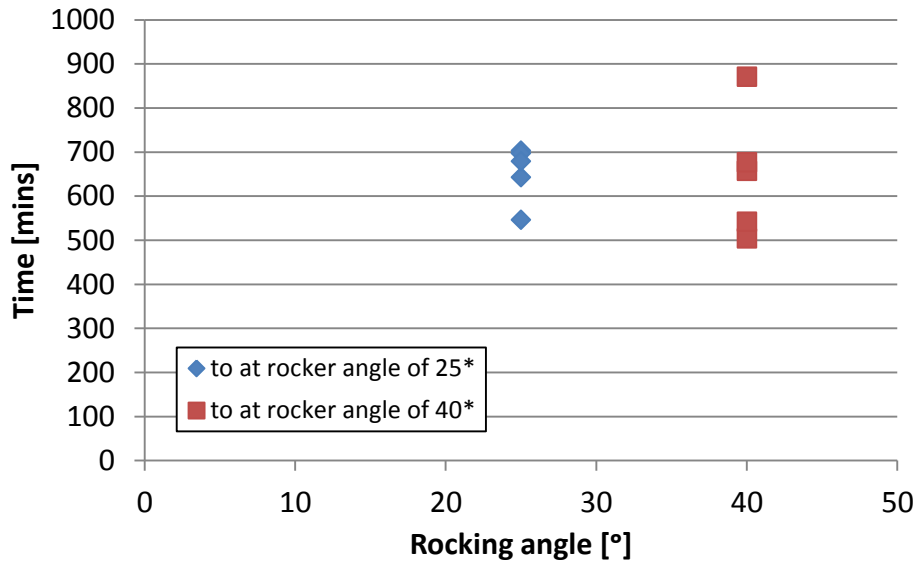

Fig. 4-11 The relationship between t_o values and different cell volumes, using Luvicap 55W at 5000 ppm.

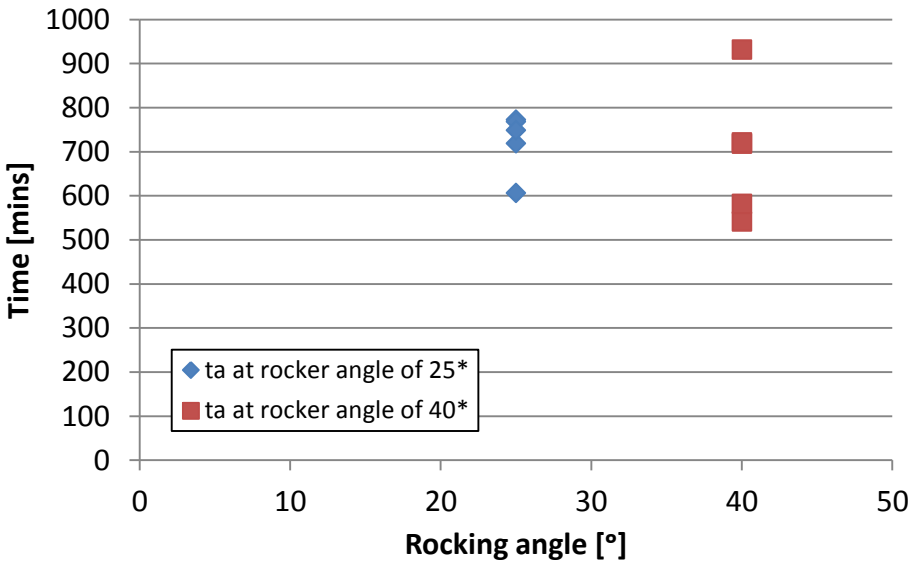

Fig. 4-12 The relationship between t_a values and different cell volumes, using Luvicap 55W at 5000 ppm.

Comments:

By changing the rocking angle for the cells, the speed of the balls will be affected. Yet the results from the experiments don't seem to change significant when the rocking angle is changed.

When the speed of the balls is reduced, the shear rates might be affected. But, as for the changes in the rocking rate; the changes might be so small that it won't affect the gas hydrate formation noticeably.

More experiments should be performed to get a better answer on how the rocking angle affects the inhibition of gas hydrates.

4.4 How the type of rocking balls will affect the results

The steel balls were replaced with rougher glass balls, and experiments were run for Luvicap 55W, Luvicap EG, Inhibex 101 and Inhibex 501 by using the constant cooling method, and for Luvicap 55W using the isothermal method.

Constant cooling method

No clear results were observed.

Results for Luvicap 55W at 2500 ppm using glass balls and steel balls can be seen graphically in Fig. 4-13 (T_o values) and in Fig. 4-14 (T_a values), and in numbers in Table 4-10.

At 2500 ppm the average T_o values were:

Glass balls : 7.4°C
Steel balls: 7.1°C

At 2500 ppm the average T_a values were:

Glass balls : 5.8°C
Steel balls : 5.8°C

When the steel balls were replaced with glass balls no statistically significant difference was observed, neither for average T_o nor average T_a.

Results for Luvicap 55W at 5000 ppm show that replacing the steel balls with glass balls would decrease average T_o and average T_a. This can be seen graphically in Fig. 4-13 (T_o values) and in Fig. 4-14 (T_a values), and in numbers in Table 4-10.

At 5000 ppm the average T_o values were:

Glass balls : 5.7°C
Steel balls : 6.6°C

At 5000 ppm the average T_a values were:

Glass balls: 3.4°C
Steel balls : 3.5°C

When the steel balls were replaced with glass balls the average T_o value decreased with 13.6%. No statistically significant difference was observed on the average T_a values.

Table 4-10 U used to make Fig. 4-13 (T_o values) and Fig. 4-14 (T_a values). The 2500 ppm steel ball experiment was performed 27.01.11, the 2500 ppm glass ball experiment was performed 21.01.11, the 5000 ppm steel ball experiment was performed 02.02.11 and the 5000 ppm glass ball experiment was performed 20.01.11. The data is taken from Appendix [A] Table of Results.

Concentration [ppm]	Ball	T_o [°C]	T_a [°C]
2500	Steel	7.0	5.9
2500	Steel	7.0	5.8
2500	Steel	7.1	5.8
2500	Steel	7.4	5.8
2500	Glass	7.0	5.8
2500	Glass	8.0	5.8
2500	Glass	6.8	5.8
2500	Glass	7.0	5.8
2500	Glass	8.0	5.8
5000	Steel	6.8	3.5
5000	Steel	6.8	3.5
5000	Steel	6.8	3.5
5000	Steel	6.2	3.3
5000	Steel	6.2	3.7
5000	Glass	5.7	3.4
5000	Glass	5.8	3.5
5000	Glass	5.4	3.2
5000	Glass	6.0	3.5
5000	Glass	5.6	3.4

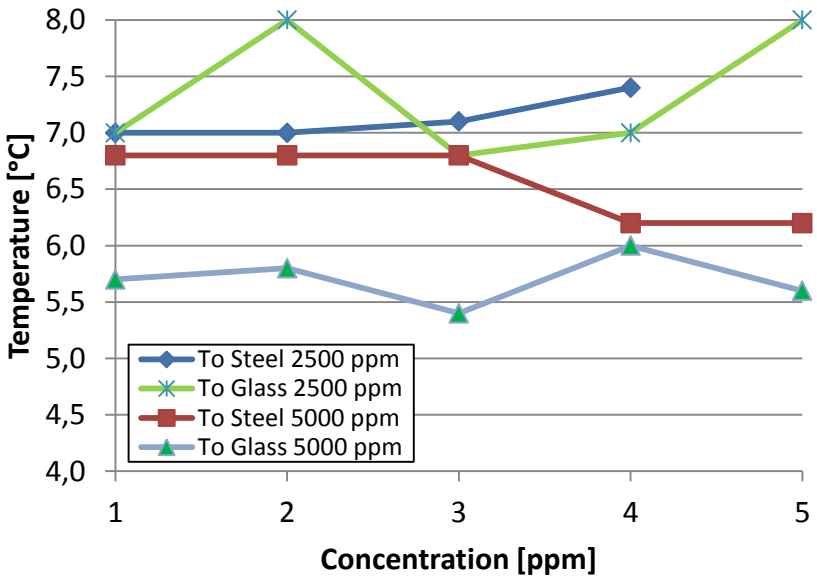

Fig. 4-13 The relationship between T_o values and different balls, using Luvicap 55W.

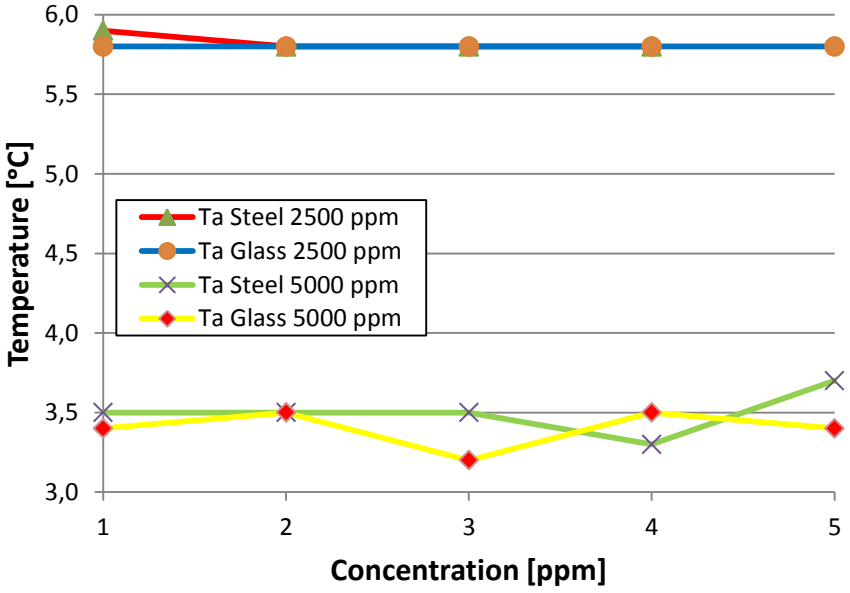

Fig. 4-14 The relationship between T_a values and different balls, using Luvicap 55W.

T_o values and T_a values using glass and steel balls for Luvicap EG, Inhibex 101 and Inhibex 501 can be found in Appendix [A] Table of Results, and a summary of the results of interests can be seen in Table 4-11.

Table 4-11 The table shows the T_o and T_a values for Luvicap EG, Inhibex 101 and Inhibex 501 at 2500 ppm and 5000 ppm tested with steel balls and glass balls. The data is taken from Appendix [A] Table of Results.

Chemical	Concentration [ppm]	Average values: T_o steel/T_o glass [°C]/[°C]	Average values: T_a steel/T_a glass [°C]/[°C]
Luvicap EG	2500	8.7/8.7	8.1/8.0
	5000	6.5/5.8	6.3/5.5
Inhibex 101	2500	7.1/5.0	2.4/2.0
	5000	No gas hydrate formation	
Inhibex 501	2500	8.4/6.9	4.9/4.6
	5000	7.1/5.0	2.4/2.0

For Luvicap EG, Inhibex 101 and Inhibex 501 are the average T_o and T_a values the same, or lower, for the tests using glass balls instead of steel balls.

No hydrates were formed using Inhibex 101 at 5000 ppm.

Isothermal method

Results for Luvicap 55W at 5000 ppm (isothermal method) show that using glass balls instead of steel balls will decrease average t_o and the average t_a. This can be seen graphically in Fig. 4-15 and Fig. 4-16, and in numbers in Table 4-12.

At 5000 ppm the average t_o values were:

Glass balls : 546 mins
Steel balls : 650 mins

At 5000 ppm the average t_a values were:

Glass balls: 601 mins
Steel balls : 699 mins

When the steel balls were replaced with glass balls the average t_o value decreased with 16.0%., and average T_a decreased with 14.0%.

Table 4-12 Data used to make Fig. 4-15 and Fig. 4-16. Steel balls and glass balls are tested at concentrations of 5000 ppm using Luvicap 55W. The steel ball experiment was performed 28.03.11, and the glass ball experiment was performed 11.04.11. Data is taken from Appendix [A] Table of Results.

Concentration [ppm]	t_o glass [mins]	t_o steel [mins]	t_a glass [mins]	t_a steel [mins]
5000	550	504	600	542
5000	647	657	691	718
5000	574	677	660	521
5000	508	871	561	932
5000	453	542	491	582

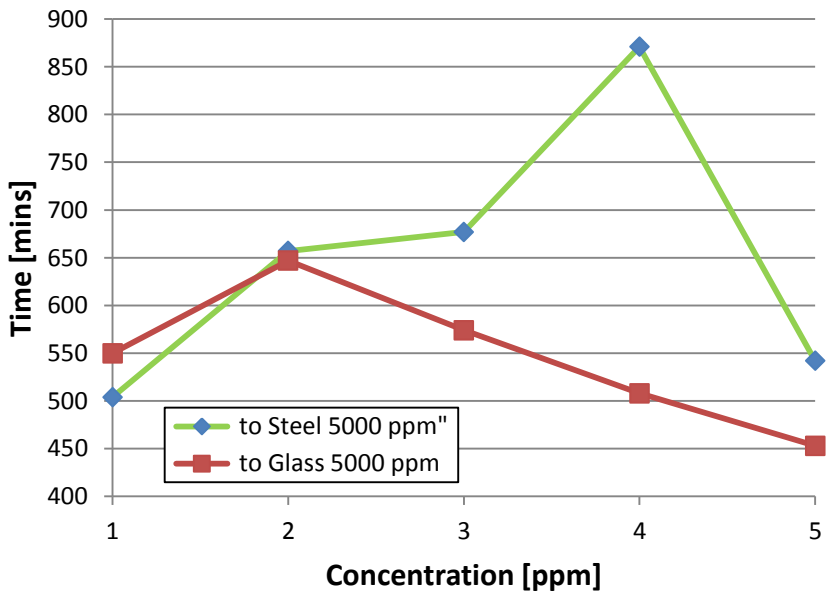

Fig. 4-15 The graph shows the time before the gas hydrate formations started, t_o using steel balls and glass balls.

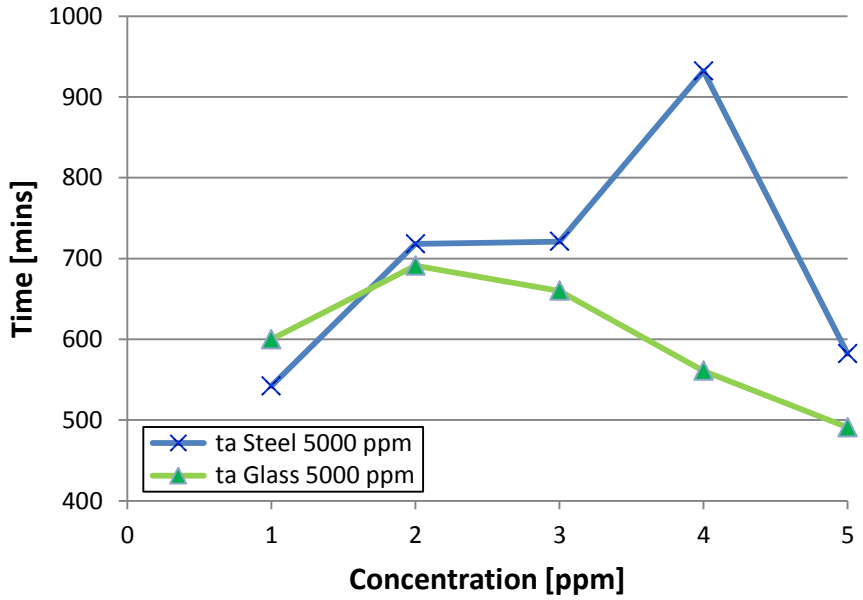

Fig. 4-16 The graph shows the time before the rapid gas hydrate formations started, t_a, using steel balls and glass balls.

Comments:

There were no clear results by replacing the steel balls with rougher glass balls. For Luvicap 55W, at 2500 ppm using the constant cooling method, the average T_o value didn't show any statistically significant difference using steel or glass balls, the average T_a value decreased with 13.6% at 5000 ppm.

Using the isothermal method (Luvicap 55W at 5000 ppm), the average t_o value decreased with 16% as the steel balls were replaced with glass balls. The biggest difference was seen using the isothermal method.

Experiments using Luvicap EG show no statistically significant difference in average T_o (using glass vs. steel balls).

Inhibex 101 and Inhibex 501 show a decrease in average T_o when changing the steel balls to glass balls.

More experiments should be performed to get a clearer answer on how the type of ball affects the inhibition of gas hydrates.

4.5 How the concentration of KHIs affects the results

The concentration of Luvicap 55W was tested at 1000 ppm, 2500 ppm (only for constant cooling method), 5000 ppm and 10000 ppm.

Constant cooling method

Results show that an increase of concentration lead to a decrease in average T_o and a decrease in average T_a. This can be seen graphically in Fig. 4-17 (T_o) and in Fig. 4-18 (T_a), and in numbers in Table 4-13.

Average T_o values were:

At 1000 ppm : 10.2°C
At 2500 ppm : 7.1°C
At 5000 ppm : 6.6°C
At 10000 ppm: 5.2°C

Average T_a values were:

At 1000 ppm : 9.2°C
At 2500 ppm : 5.8°C
At 5000 ppm : 3.5°C
At 10000 ppm: 2.0°C

When the concentration was reduced from 2500 ppm to 1000 ppm, the average T_o value decreased with 43.7%. The corresponding average T_a value decreased with 58.6%.

When the concentration was increased from 2500 ppm to 5000 ppm, the average T_o value increased with 7.0%. The corresponding average T_a value increased with 39.7%.

When the concentration was increased from 5000 ppm to 10000 ppm, the average T_o value increased with 21.2%. The corresponding average T_a value increased with 42.9%.

Table 4-13 Data used to make Fig. 4-17 and Fig. 4-18. The concentration is Luvicap 55W in distilled water. The experiments were performed 09.04.11 (1000 ppm), 27.01.11 (2500 ppm), 02.02.11 (5000 ppm) and 10.04.11 (10000 ppm). The data is extracted from Appendix [A] Table of Results.

Concentration [ppm]	To [°C]	Ta [°C]
1 000	10.3	9.7
1 000	9.4	9.0
1 000	10.8	10.0
1 000	10.0	9.6
1 000	10.4	9.3
2 500	7.0	5.9
2 500	7.0	5.8
2 500	7.1	5.8
2 500	7.4	5.8
5 000	6.8	3.5
5 000	6.8	3.5
5 000	6.8	3.5
5 000	6.2	3.3
5 000	6.2	3.7
10 000	4.3	2.0
10 000	6.2	2.0
10 000	6.3	2.0
10 000	4.3	2.0
10 000	4.8	2.2

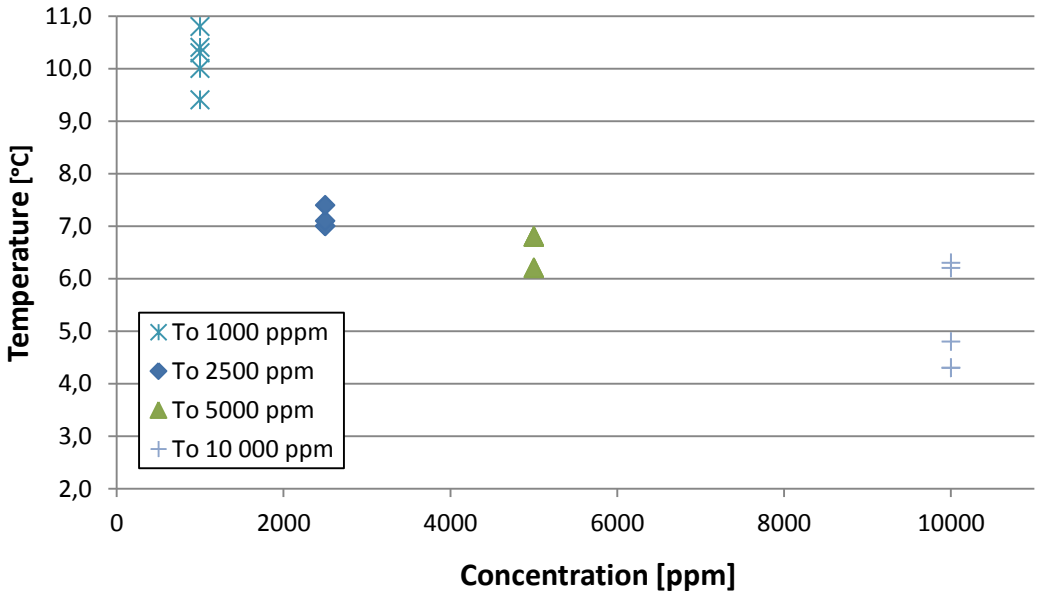

Fig. 4-17 The relationship between T_o values and different concentrations.

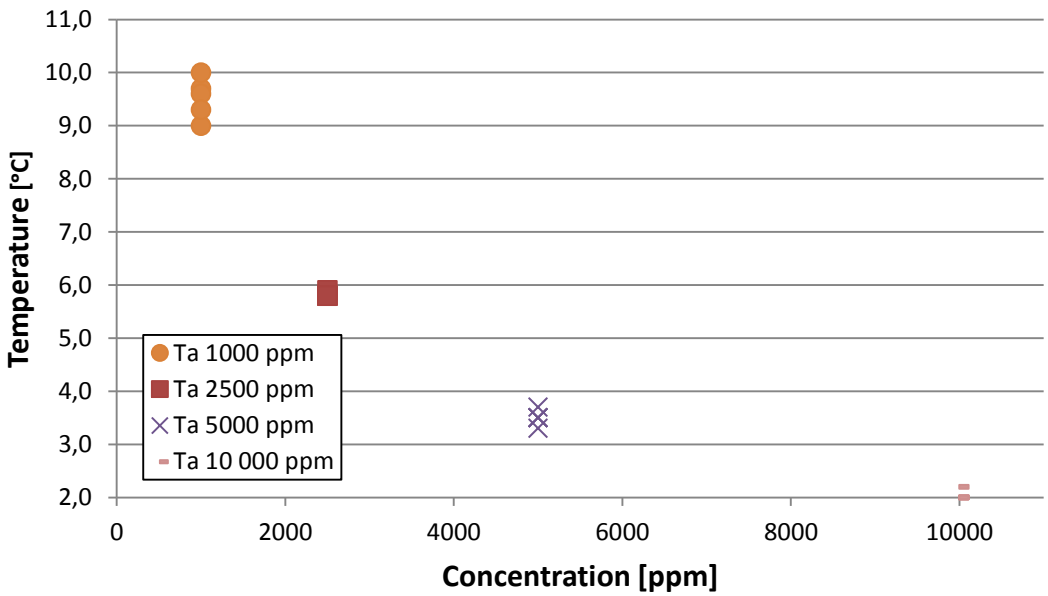

Fig. 4-18 The relationship between T_a values and different concentrations.

Isothermal method

At 1000 ppm the hydrates started to form before 7°C was reached.

Results show that an increase of concentration lead to an increase in average t_o and an increase in average t_a. This can be seen graphically in Fig. 4-19 (t_o) and Fig. 4-20 (t_a), and in numbers in Table 4-14.

Average t_o values were:

At 1000 ppm : 0 mins
At 5000 ppm : 650 mins
At 10000 ppm: 1048 mins

Average t_a values were:

At 1000 ppm : 8 mins
At 5000 ppm : 699 mins
At 10000 ppm: 1189 mins

When the concentration was reduced from 5000 ppm to 1000 ppm, the average t_a value decreased with 98.9%.

When the concentration was increased from 5000 ppm to 10000 ppm, the average t_o value increased with 61.2%. The corresponding average t_a value increased with 70.1%.

Table 4-14 Data used to make Fig. 4-19 and Fig. 4-20. The concentration is Luvicap 55W in distilled water. The experiments were performed 07.04.11 (1000 ppm), 28.03.11 (5000 ppm) and 08.04.11 (10000 ppm). The data is extracted from Appendix [A] Table of Results.

Concentration [ppm]	t_o [mins]	t_a [mins]
1 000	0	10
1 000	0	7
1 000	0	13
1 000	0	7
1 000	0	5
5 000	504	542
5 000	657	718
5 000	677	721
5 000	871	932
5 000	542	582
10 000	1043	1163
10 000	1243	1503
10 000	993	1123
10 000	1084	1159
10 000	877	998

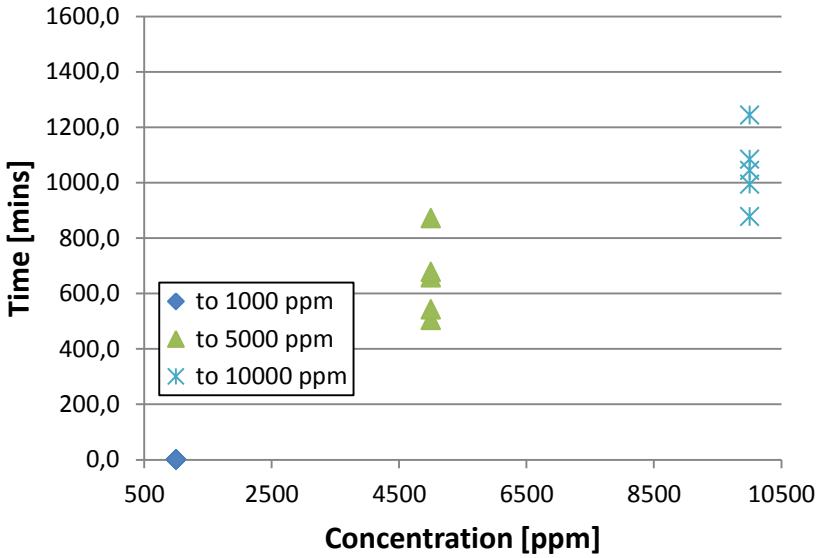

Fig. 4-19 The relationship between t_o values and different concentrations.

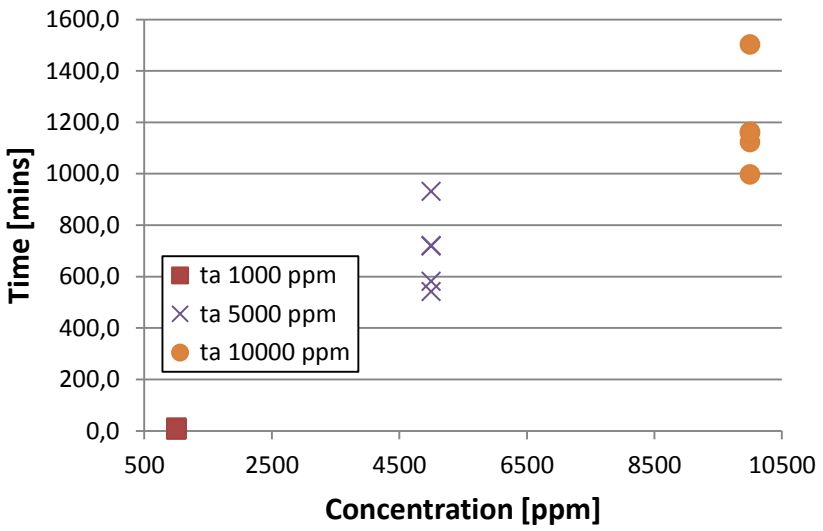

Fig. 4-20 The relationship between t_a values and different concentrations.

Comments:

The results fits the theory; as more inhibitor added to the system, more water is prevented from participating in the hydrate structure and higher pressure and lower temperatures are required for gas hydrate formation from the remaining uninhibited water (Sloan 2011).

4.6 How the molecular weight of the KHIs affects the result

According to literature, the molecular weight will impact the ability of a chemical to inhibit the gas hydrate formation. There are too few interactions with the hydrate surface per polymer chain to cause any inhibition when the molecular weight is too low. As the molecular weight increases, there will be a decrease in the number of polymer strands in solution, and some of the alkylamide side chains may become less available for interaction with hydrate surfaces (Kelland, Svartås et al. 2000). At increasing molecular weights the performance drops slowly, but it won't disappear (Del Villano 2009).

In section 2.2.2 Kinetic Hydrate Inhibitors it is said that the ideal molecular weight for a KHI polymer usually is around 1500-3000 (Del Villano 2009).

The results can be seen graphically in Fig. 4-21, and in numbers in Table 4-15 and seem to fit the theory.

Table 4-15 Data used to make Fig. 4-21. The concentration is 5000 ppm for the inhibitors. The tests were performed 28.02.11 (PVP Plasdone), 02.05.11 (PVP 30k) and 01.03.11 (PVP 120k). The data is extracted from Appendix [A] Table of Results.

Cell number	T_o PVP Plasdone (Mw 4000) [°C]	T_o PVP 30k (Mw 60000) [°C]	T_o PVP 120k (Mw 3 mill) [°C]
1	10.3	11.3	13.4
2	10.3	13.0	13.4
3	12.0	12.8	14.0
4	12.0	12.9	13.9
5	10.8	11.0	13.2

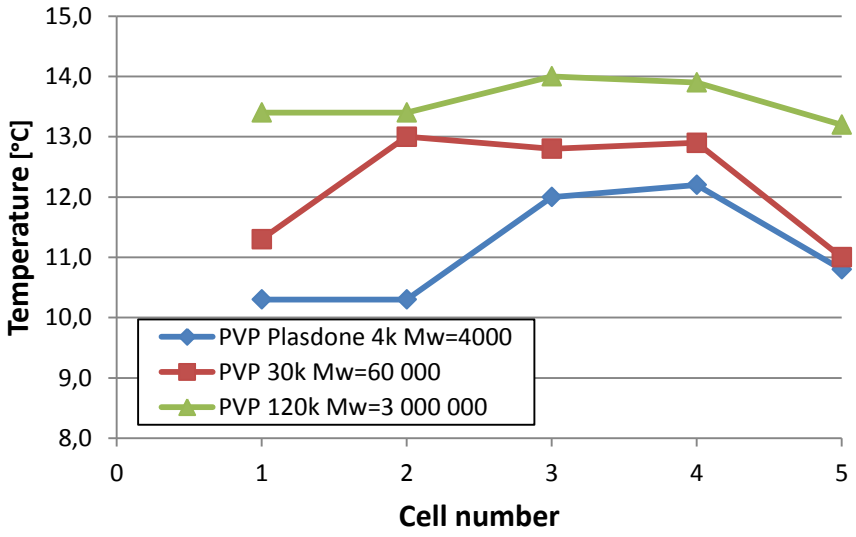

Fig. 4-21 The relationship between T_o and different molecular weights for PVPs.

4.6 How adding of synergist affects the results

Polymers of two classes can be blended in order to obtain a synergistic action (Clark and Anderson 2007; Huang, Wang et al. 2007). Luvicap EG was mixed with TBAB (Tetra Butylammonium Bromide) which is a synergist (Duncum, Edwards et al. 1996). The concentration was 2500 ppm with a ratio of 1:1. It was expected that the performance of Luvicap EG would improve, which it did.

The results show that adding TBAB to Luvicap EG causes to a decrease in average T_o, and a decrease in average T_a. This can be seen graphically in Fig. 4-22 (T_o) and Fig. 4-23 (T_a) and in numbers in Table 4-16.

When TBAB was added to Luvicap EG, the average T_o value decreased with 23.9%. The corresponding average T_a value decreased with 24.6%.

Table 4-16 Data used to make Fig. 4-22 and Fig. 4-23. The concentration of Luvicap EG in a mixture with TBAB is 2500 ppm, with a ratio of 1:1. The experiments were performed 10.01.11 (Luvicap EG) and 07.02.11 (Luvicap EG + TBAB). The data is extracted from Appendix [A] Table of Results.

Cell number	Luvicap EG T_o [°C]	Luvicap EG + TBAB T_o [°C]	Luvicap EG T_a [°C]	Luvicap EG + TBAB T_a [°C]
1	8.1	6.3	7.9	5.9
2	9.3	7.0	8.0	6.2
3	8.8	6.8	8.0	6.2
4	8.7	7.0	8.2	6.2
5	8.7	6.1	8.2	5.9

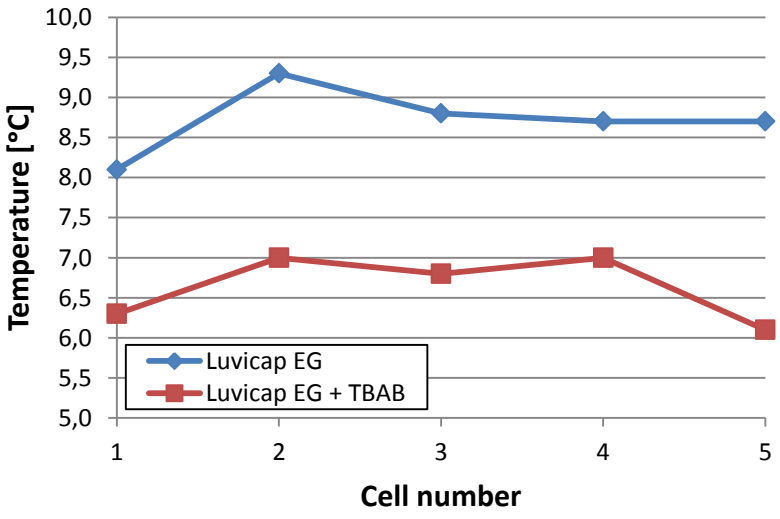

Fig. 4-22 The relationship between T_o values and Luvicap EG with and without a synergist, at 2500 ppm.

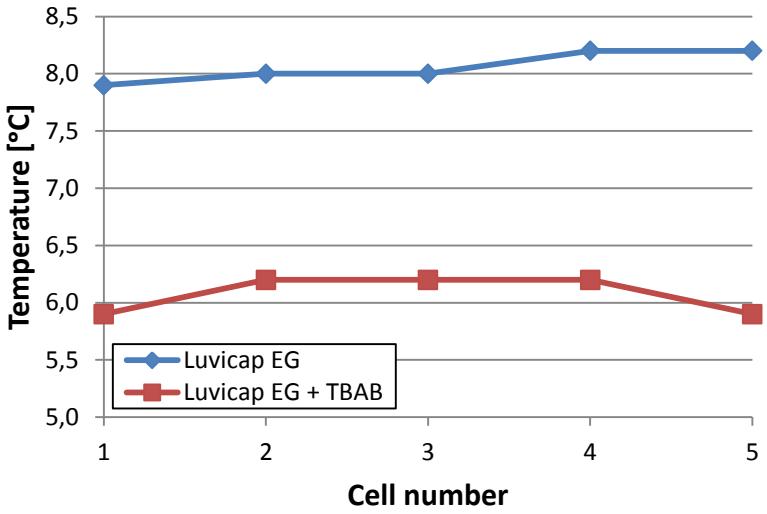

Fig. 4-23 The relationship between T_a values and Luvicap EG with and without a synergist, at 2500 ppm.

Luvicap EG was mixed with BGE (Butyl Glycol Ether) to check if this would improve the inhibition. The reason for doing this is that ISP's Inhibex 101 is PVCAP in BGE solvent. It is claimed that BGE improves the performance of the PVCap, and to be "fair" to BASF who make Luvicap EG (PVCap in ethylene glycol), their PVCap was tested with BGE. The ratio of Luvicap EG and BGE were 1:1, and they were tested at 2500 ppm and 5000 ppm. The results from the experiments can be found in Appendix [A] Table of Results.

At 2500 ppm the average T_o values were:

Luvicap EG : 8.7°C
Luvicap EG + BGE : 7.4°C

At 2500 ppm the average T_a values were:

Luvicap EG : 8.1°C
Luvicap EG + BGE : 4.0°C

When BGE was added to Luvicap EG (ratio 1:1, 2500 ppm), the average T_o value decreased with 14.9%. The average T_a value decreased with 50.6%.

At 5000 ppm the average T_o values were:

Luvicap EG : 6.5°C
Luvicap EG + BGE : 3.2°C

At 5000 ppm the average T_a values were:

Luvicap EG : 6.3°C
Luvicap EG + BGE : 2.7°C

When BGE was added to Luvicap EG (ratio 1:1, 5000 ppm) average T_o value decreased with 50.8%. The average T_a value decreased with 57.1%.

4.7 Possible conditioning of the cells

Some of the results found in these experiments gave a reason to believe that there have been conditionings of the cells. This means that the results from an experiment run in December will vary from the results from the same experiment run later, for example in February/March, due to manufacturing impurities or that the inside of the cells have lost some of its roughness.

Experiments using only distilled water were performed under same conditions 02.12.2010 and 01.02.2011. The graphically results are shown in Fig. 4-24, and in numbers in Table 4-17.

Table 4-17 Data used to make Fig. 4-24. The experiment is run using distilled water only. The data is extracted from Appendix [A] Table of Results.

Cell number	T_o [°C] 02.12.2010	T_o [°C] 01.02.2011
1	18.9	17.4
2	18.5	17.2
3	18.2	17.5
4	18.3	17.2
5	18.8	18.6

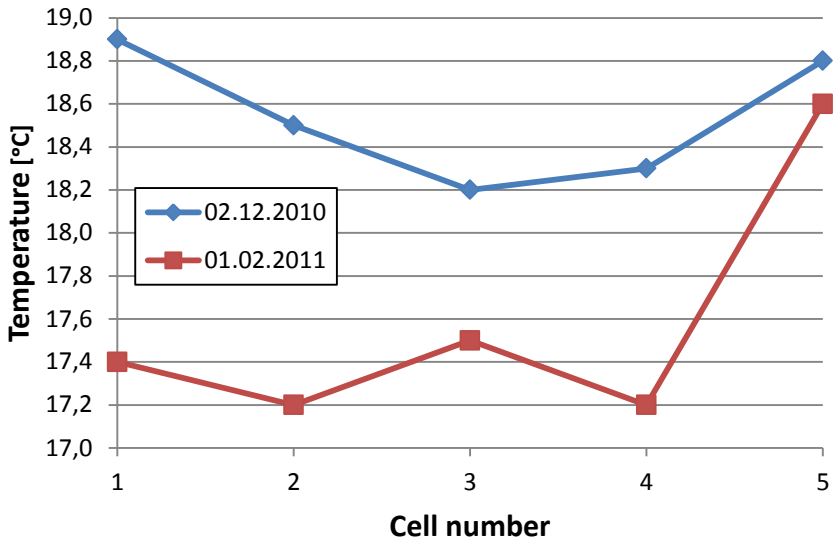

Fig. 4-24 Possible conditioning of the cells. The experiment is run using distilled water.

Average T_o values are:

02.12.2010 : 18.5 °C
01.02.2011 : 17.6 °C

Average T_o was reduced with 24.3% from December 2010 to February 2011.

Experiments using Luvicap 55W (5000 ppm) were performed under same conditions 03.12.2010 and 04.03.2011. The graphically results are shown in Fig. 4-25, and in numbers in Table 4-18.

Table 4-18 Data used to make Fig. 4-25. The experiment is run using Luvicap 55 (5000 ppm). The data is extracted from Appendix [A] Table of Results.

Cell number	T_o [°C] 03.12.2010	T_o [°C] 04.03.2011
1	6.9	6.3
2	7.0	6.2
3	7.4	6.1
4	6.5	6.1
5	6.5	6.5

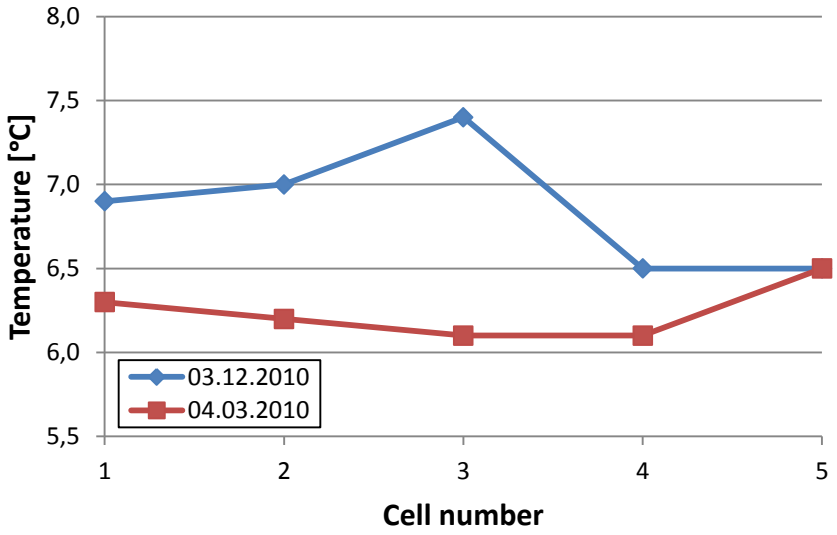

Fig. 4-25 Possible conditioning of the cells. Luvicap 55W (5000 ppm) is used.

Average T_o values are:

03.12.2010 : 6.9 °C
04.03.2011 : 6.2 °C

Average T_a values are:

03.12.2010 : 4.1 °C
04.03.2011 : 3.4 °C

The average T_o was reduced with 10.1% from December 2010 to March 2011.

The average T_a was reduced with 17.1% from December 2010 to March 2011.

Experiments using Inhibex 101 (2500 ppm) were performed under same conditions 09.12.2010 and 22.02.2011. The graphically results are shown in Fig. 4-26, and in numbers Table 4-19.

Table 4-19 Data used to make Fig. 4-26. The experiment is run using Inhibex 101. The data is extracted from Appendix [A] Table of Results

Cell number	T_o [°C] 09.12.2010	T_o [°C] 22.02.2011
1	7.0	5.0
2	7.2	5.0
3	5.7	4.8
4	5.6	5.2
5	5.2	4.2

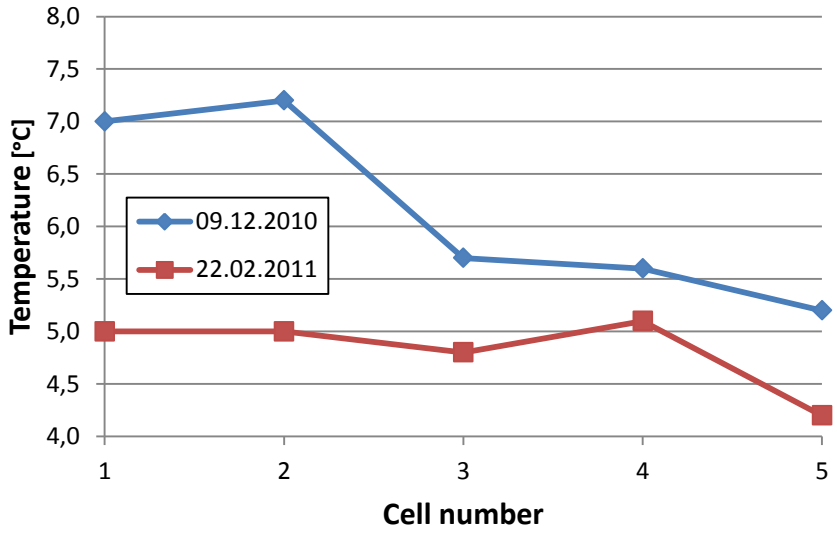

Fig. 4-26 Possible conditioning of the cells. Inhibex 101 (2500 ppm) is used.

Average T_o values are:

09.12.2010 : 6.1 °C
22.02.2011 : 4.8 °C

Average T_a values are:

09.12.2010 : 3.3 °C
22.02.2011 : 3.1 °C

The average T_o was reduced with 21.3% from December 2010 to February 2011.

The average T_a was reduced with 6.1% from December 2010 to February 2011.

Comments:

For all the experiments presented above, T_o and T_a values have decreased from the early experiments to the same experiments run later. There might seem as if there has been conditioning of the cells.

4.8 The reproducibility of the results

The scattering based on the deviation from the results of each cell compared to the average value for the experiment is calculated to find the reproducibility. The calculations are found in Appendix [B] Percentage Deviation From Average, and a summary of the results are presented in Table 4-20.

KHI experiments using small, sapphire steel cells do usually obtain a scattering in the induction times of about 40-50% using the isothermal method (Del Villano and Kelland 2009). From the University of Stavanger its reported that the scatter in hold time using non-precursor methods generally is about 30-40% on either side of the average of a series (Del Villano and Kelland 2009).

Using the RC5, constant cooling method, most of the deviations are < 10%. From Table 4-20 and Appendix [B] Percentage Deviation From Average, only 9.6% of the reported values divagates from the average with < 10%.

Using the RC5, isothermal method, the deviations are higher compared to using constant cooling method, as 46.6% of the reported values divagates from the average with <10%.

The average deviations are 4.4% using the constant cooling method, and 16.2% using the isothermal method.

Table 4-20 The deviations for each cell compared to average using the constant cooling method and the isothermal method.

Cooling method	Average deviation	Maximum deviation	Deviation of more than 10%	Deviation of more than 20%	Deviation of more than 30%
Constant cooling method	4.4%	25.7%	9.6%	1.6%	0%
Isothermal method	16.2%	134.9%	46.6%	22.3%	16.9%

It can be concluded, based on Table 4-20, it can be concluded that RC5 provides reliable results.

4.9 The results from RC5 compared to literature

From Table 4-21 and the equilibrium curve in Fig. 4-27 using SNG (Synthetic Natural Gas) and distilled water, the subcooling at 77 bar is ca. 19.8°C. According to the Appendix [A] Table of Results, hydrates started to form at 18.5°C in December 2010 and 17.6°C in February 2011. The results from experiments using the RC5 are lower than expected based on literature.

Table 4-21 Data used to make Fig. 4-27 Hydrate PT curve from UiS SNG (Synthetic Natural Gas), DI water, calculated by PVTSim software from Calsep, Denmark.

Temperature [°C]	Pressure [bar]
0	6.25
3.1	8.06
5.1	10.35
7.1	13.27
9.1	17.00
11.1	21.82
13.1	28.15
15.1	36.67
16.82	46.67
18.11	56.67
19.10	66.67
19.89	76.67
20.52	86.67
21.04	96.67
21.48	106.67
21.88	116.67
21.99	120.00

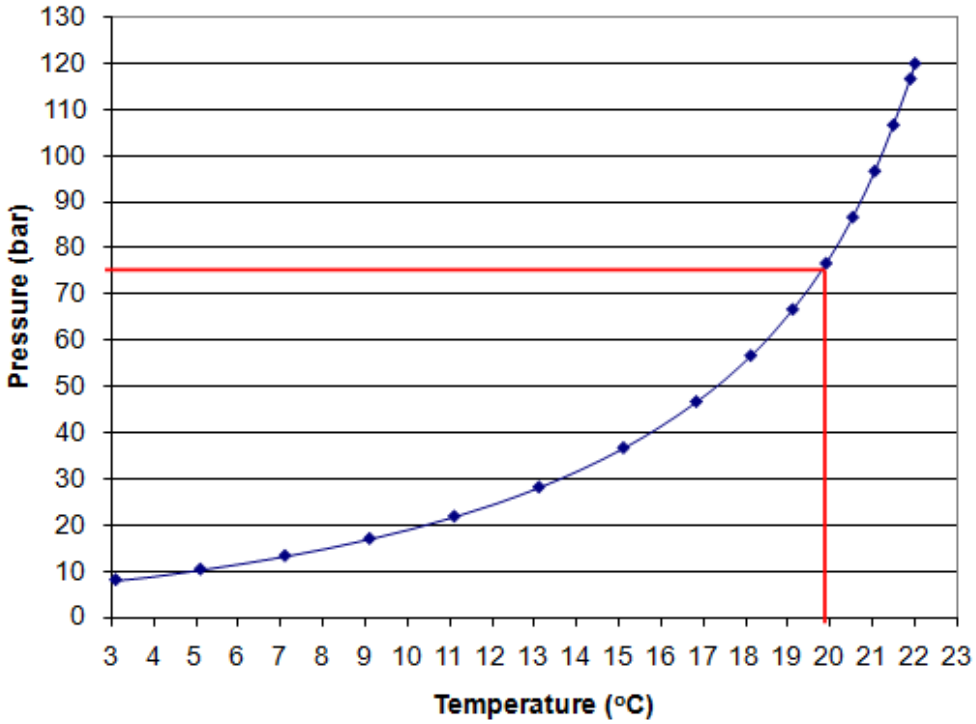

Fig. 4-27 Hydrate PT curve from UiS SNG (Synthetic Natural Gas), DI water, calculated by PVTSim software from Calsep, Denmark.

4.10 Ranking of the chemicals

The chemicals were ranked according to their performances on inhibiting gas hydrate formations using both the constant cooling method and the isothermal method. The results from the experiments can be seen graphically in Fig. 4-28, Fig. 4-29, Fig. 4-30, Fig. 4-31, Fig. 4-32 and Fig. 4-33. The cooling method and concentrations are varied. The figures are made based on information in Table 4-22.

The results show that Inhibex 101 is the best chemical to prevent/postpone gas hydrate formation under all experiment conditions.

The total ranking can be seen in Table 4-23.

Table 4-22 Data used to make Fig. 4-28, Fig. 4-29, Fig. 4-30, Fig. 4-31, Fig. 4-32 and Fig. 4-33. The data is taken from Appendix [A] Table of Results.

Chemical	Constant cooling method 2500 ppm T_o/T_a [°C]/[°C]	Constant cooling method 5000 ppm T_o/T_a [°C]/[°C]	Isothermal method 5000 ppm t_o/t_a [mins]/[mins]
Luvicap 55W	7.1/5.8	6.6/3.5	589/660
Luvicap EG	8.7/8.1	6.5/6.3	113/141
Inhibex 101	4.8/3.1	3.1/-	1278/1296
Inhibex 501	8.4/4.9	7.1/2.4	113/116

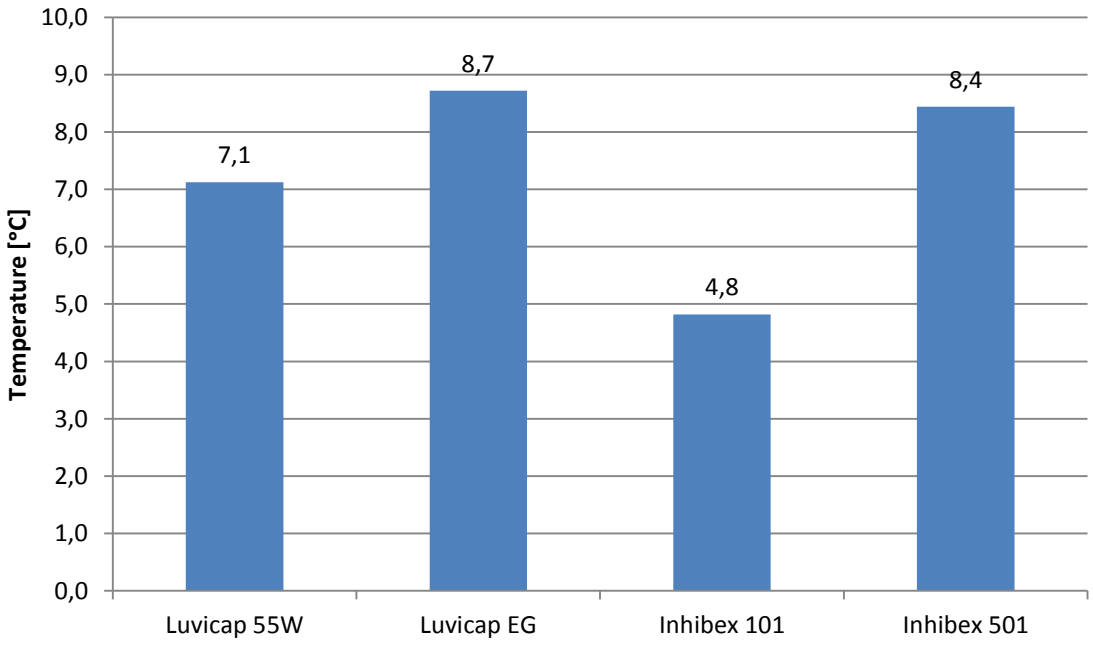

Fig. 4-28 Constant cooling method. The chemicals are ranked based on average T_o values at 2500 ppm.

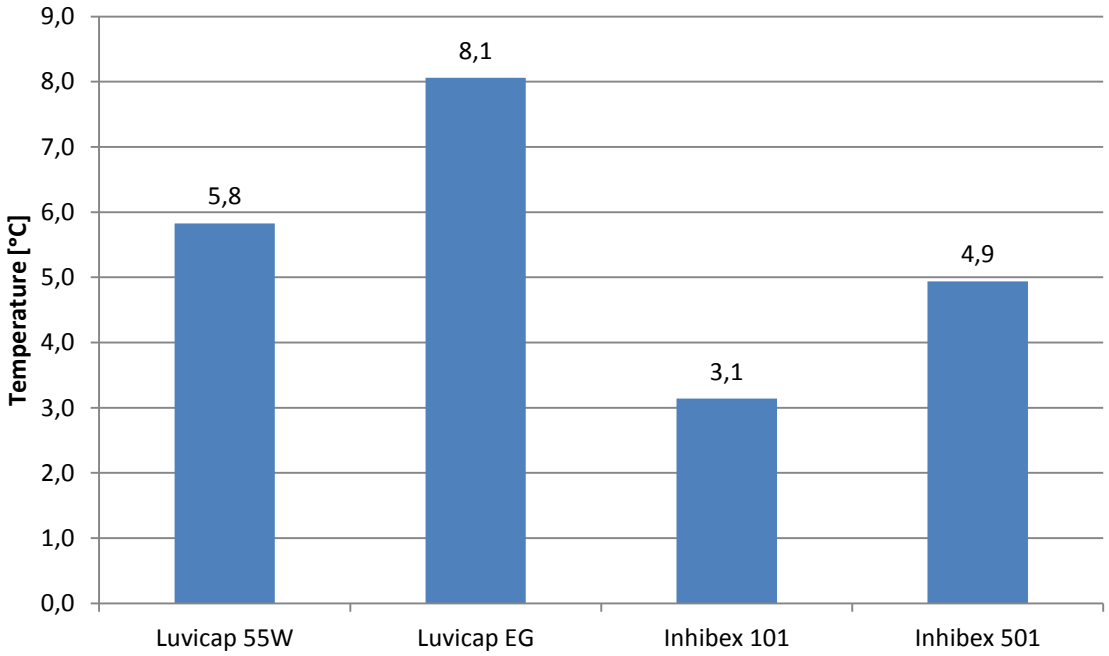

Fig. 4-29 Constant cooling method. The chemicals are ranked based on average T_a values at 2500 ppm.

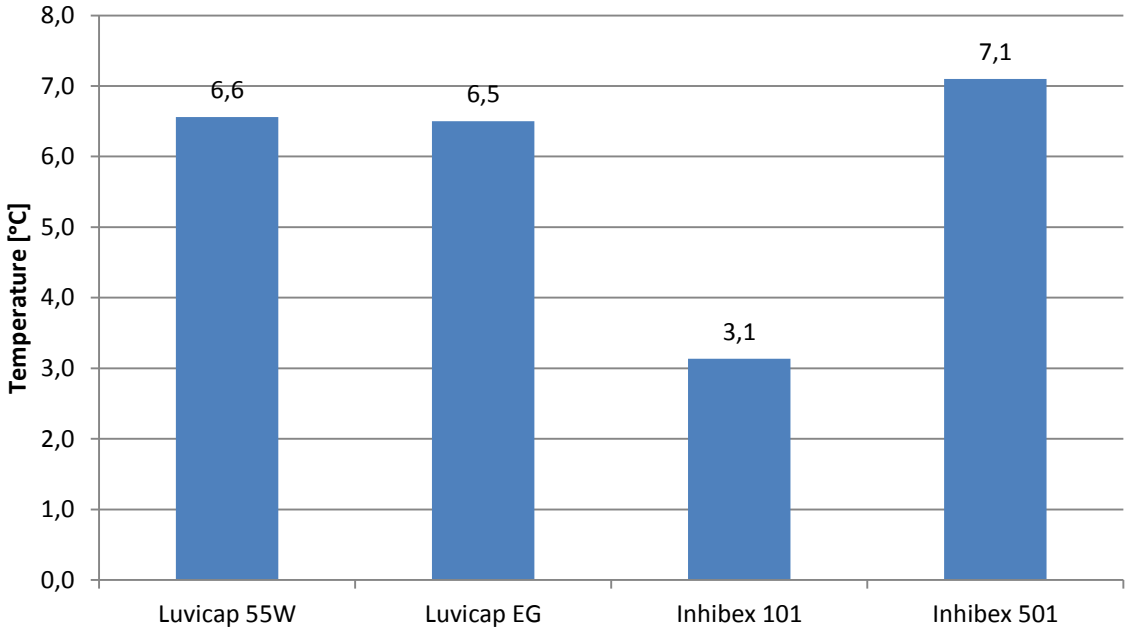

Fig. 4-30 Constant cooling method. The chemicals are ranked based on average T_o values at 5000 ppm.

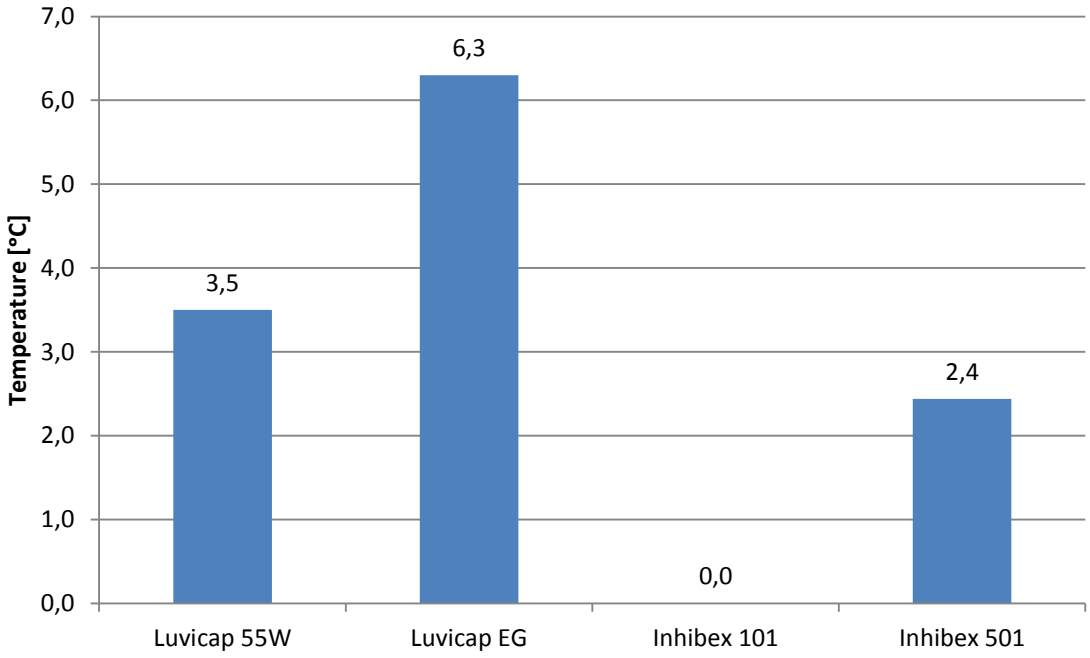

Fig. 4-31 Constant cooling method. The chemicals are ranked based on average T_a values at 5000 ppm.

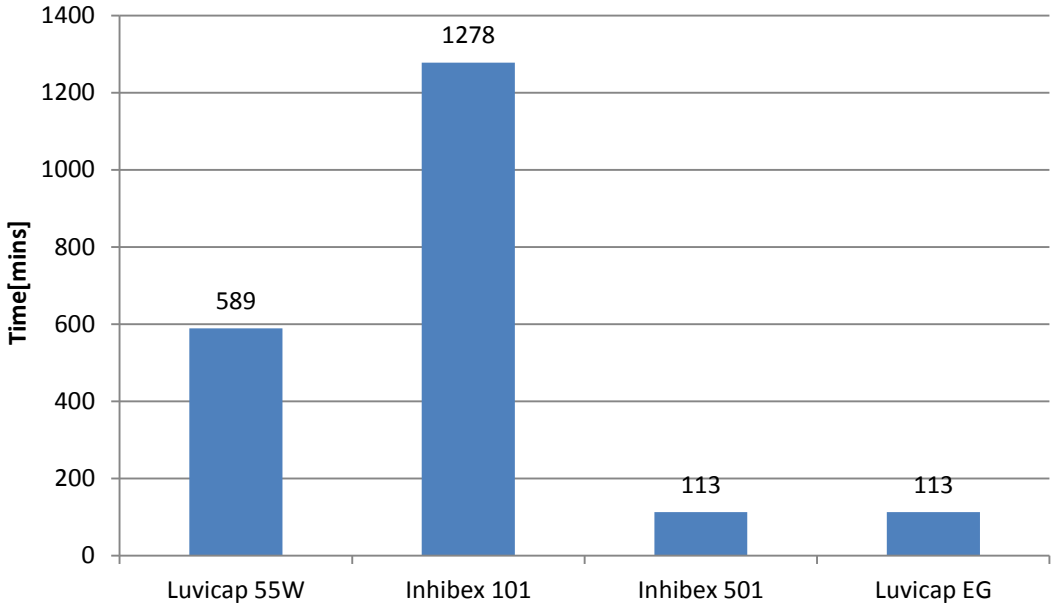

Fig. 4-32 Isothermal method, 7°C. The chemicals are ranked based on average t_o values at 5000 ppm.

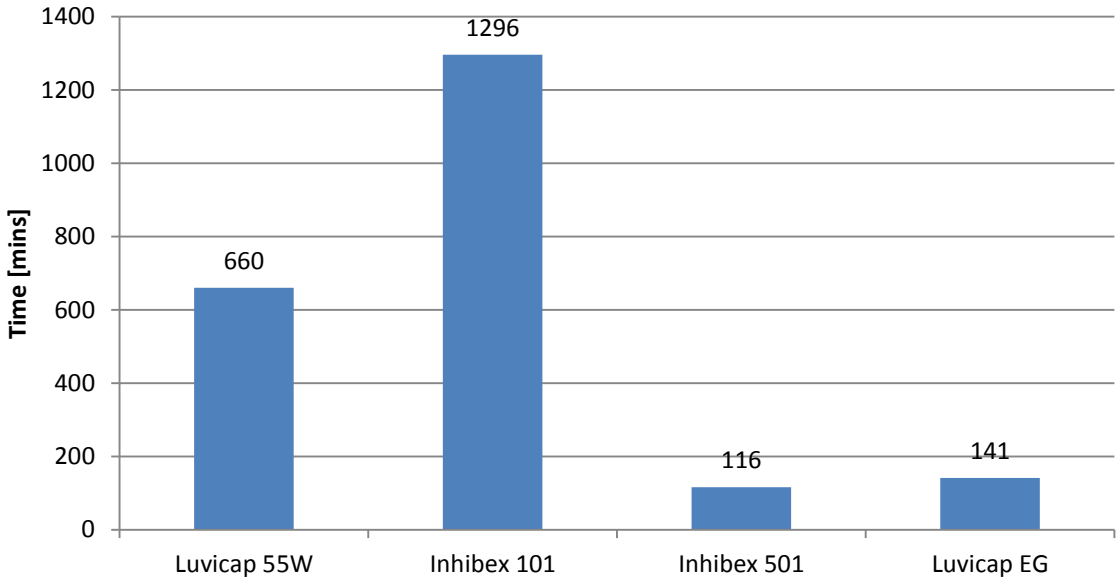

Fig. 4-33 Isothermal method, 7°C. The chemicals are ranked based on average t_a values at 5000 ppm.

Comments:

An overview of the ranking of the chemicals can be seen in Table 4-23.

Since the experiments run over a long period of time (5 months) possible conditioning of the cells may have impacted the results when it comes to ranking the inhibitors. The experiments using the isothermal method are all performed in March/April, and conditioning of the cells have not impacted these results.

Inhibex 101 is the better inhibitor during all the experiments presented in Table 4-22. As explained earlier, Inhibex 101 and Inhibex 501 are mixed with BGE (which is said to act as a synergist) and may be part of the solution why one of these ranks as the better inhibitor.

The molecular weight of Inhibex 101 is from 2000-5000, and, also mentioned earlier, for optimal performances, the ideal molecular weight for a KHI polymer is usually around 1500-3000 (Del Villano 2009). This explains the advantage Inhibex 101 has compared to Inhibex 501 with a molecular weight of 5000-8000.

More experiments should be performed to be able to rank the kinetic hydrate inhibitors using the RC5.

Table 4-23 Ranking based on average values for Luvicap 55W, Luvicap EG, Inhibex 101 and Inhibex 501 using isothermal method (at 5000ppm) and constant cooling method (at 2500 ppm and 5000 ppm).

Cooling method and inhibitor concentration	Rank	Inhibitor
Constant cooling 2500 ppm Based on average T_o values		
Fig. 4-28	1	Inhibex 101
	2	Luvicap 55W
	3	Inhibex 501
	4	Luvicap EG
Constant cooling 2500 ppm Based on average T_a values		
Fig. 4-29	1	Inhibex 101
	2	Inhibex 501
	3	Luvicap 55W
	4	Luvicap EG
Constant cooling 5000 ppm Based on average T_o values		
Fig. 4-30	1	Inhibex 101
	2	Luvicap EG
	3	Luvicap 55W
	4	Inhibex 501
Constant cooling 5000 ppm Based on average T_a values		
Fig. 4-31	1	Inhibex 101
	2	Inhibex 501
	3	Luvicap 55W
	4	Luvicap EG
Isotherm at 7°C 5000 ppm Based on average t_o values		
Fig. 4-32	1	Inhibex 101
	2	Luvicap 55W
	3	Luvicap EG/Inhibex 101
	4	Luvicap EG/Inhibex 101
Isotherm at 7°C 5000 ppm Based on average t_a values		
Fig. 4-33	1	Inhibex 101
	2	Luvicap 55W
	3	Luvicap EG
	4	Inhibex 501

5. Conclusion

A standard procedure has been established using the RC5 to test KHIs. The initial pressure for all the experiments is 77 bar. The reproducibility of the experiments is very good, and using the RC5 is a clean and simple way of testing inhibitors under pressure.

Results indicate that there has been a conditioning of the cells since the start-up in December. This might be because of manufacturing impurities or that the inside of the cells have lost some of its roughness. Average T_o value for distilled water tested in February was 4.9% lower than the average T_o value for an experiment in December. It is recommended that the results from the first weeks are discarded. Possible conditioning of the cells might have affected the results and the validation of the comparison of how the parameters affect the results.

The average T_o value found by testing distilled water in the RC5 was compared to an equilibrium curve for synthetic natural gas and distilled water calculated by Calsep's PVTSim program. The experimental T_o values were lower than the values from Calsep's PVTSim program. In February was the average T_o 11.6% lower than the value from Calsep's.

Experiments show that the gas hydrate inhibition improved as the aqueous liquid volume increased. This is valid both using the constant cooling method and the isothermal method.

The impact of the rocking rate is not clear and more experiments should be performed to get a better answer on how the rocking rate affects the inhibition of gas hydrates.

The rocking angle does not seem to impact the results, as no statistically significant difference was observed. More tests should be run to check the validity of this conclusion.

The type of ball used for the experiments does not show any clear results. By using the constant cooling method to test Luvicap 55W the average T_a value didn't show any statistically significant difference at 2500 ppm, while at 5000 ppm the average T_a value increased with 13.6%.

Using the isothermal method, the induction time decreased when the steel balls were replaced with glass balls.

The concentration is directly correlated with the effect of the hydrate inhibitor; higher concentrations gives lower T_o and T_a values, and higher t_o and t_a values, and better inhibition of gas hydrates.

A synergist (TBAB) was added to Luvicap EG (ratio 1:1), and the inhibition effect (based on average T_o and T_a values) increased with ca. 24% compared to the average values using Luvicap EG alone.

Luvicap EG was also added BGE (ratio 1:1), and as predicted did BGE improve the inhibition effect, average T_o dropped with 50.8% compared to experiments using only Luvicap EG.

The reproducibility is very good as the scatter, based on deviations from the results from each cell compared to the average of all cells (in the same experiment), is 4.4 using the constant cooling method, and 16.9% using the isothermal method.

The ranking of the chemicals, based on how they inhibit hydrate growth (T_o, T_a, t_o and t_a values) does not give the same results when using constant cooling method and isothermal method. The exception is Inhibex 101 which is the best inhibitor under all test conditions.

Future work and experiments are recommended in order to check the validity of these conclusions.

Further work should include using liquid hydrocarbon instead of gas, testing the effect of salinity (which affects subcooling) and testing the effect of pressure (which also affects subcooling). How the presence of Zalo or other surfactants (e.g. silica, sandstone, clay, chalk or scale) will affect the results, as well as the influence of pH, should also be determined.

The rocker rig, if used properly, can give reliable results for ranking KHIs. As several tests can be conducted simultaneously, results will be gained in less time than using autoclaves.

Appendix

[A] Table of Results

[B] Percentage Deviation From Average

[C] Calculations

References

Ajiro, H., Y. Takemoto, et al. (2010). Energy and Fuels **24**: 6400.

Anklam, M. R., D. J. York, et al. (2008). "Effects of Antiagglomerants on the Interactions Beteen Hydrate Particles." AIChE Journal **54**(2).

Arjmandi, M., B. Tohidi, et al. (2005). "Is Subcooling the Right Driving Force for Testing Low-Dosage Hydrate Inhibitors?" Chemical Engineering Science **60**: 8.

Carroll, J. J. (2009). Natural Gas Hydrates: A Guide for Engineers. Amsterdam, Elsevier.

Cingotti, B., A. Sinquin, et al. (2000). Study of Methane Hydrate Inhibition Mechanisms using Copolymers. Proceedings of the 3rd International Conference on Gas Hydrates, Annals of the New York Academy of Science. **912:** 766-776.

Clark, L. W. and J. Anderson (2007). "Low Dosage Hydrate Inhibitors (LDHI): Further Advances and Development in Flow Assurance Technology and Applications Concerning Oil and Gas Production Systems." IPTC 11538, International Petroleum Technology Conference.

Cohen, J. M., P. F. Wolf, et al. (1998). "Enhanced Hydrate Inhibitors: Oowerful Synergism with Glycol Ethers." Energy and Fuels **12**: 2.

Colle, K. S., R. H. Oelfk, et al. (1999). US Patent 5874660.

Deaton, W. M. and E. M. Frost (1937). Oil Gas J. **36**: 75.

Del Villano, L. (2009). Studies on Biodegradable Kinetic Hydrate Inhibitors. Stavanger, UiS. **no. 88:** 1 b. (flere pag.).

Del Villano, L. and M. A. Kelland (2009). An Investigation into the Gas Hydrate Precursor Test Method for the Laboratory Evaluation of the Performance of Kinetic Hydrate Inhibitors. Studies on Biodegradable Kinetic Hydrate Inhibitors. L. Del Villano. Stavanger, UiS.

Del Villano, L. and M. A. Kelland (2009). An Investigation into the Kinetic Hydrate Inhibitor Properties of two Imidazolium-Based Ionic Liquids on Structure II Gas Hydrates. Studies on Biodegradable Kinetic Hydrate Inhibitors. L. Del Villano. Stavanger, UiS.

Del Villano, L. and M. A. Kelland (2011). "An Investigation into the Laboratory Method for the Evaluation of the Performance of Kinetic Hydrate Inhibitors using Superheated Gas Hydrates." Chemical Engineering Science **66**.

Del Villano, L., R. Kommedal, et al. (2009). Energy and Fuels **23**.

Del Villano, L., R. Kommedal, et al. (2008). Energy and Fuels **22**.

Duncum, S., A. R. Edwards, et al. (1996). WO Patent Application 96/04462.

E. Dendy Sloan, J. (1997). Clathrate Hydrates of Natural Gases. New York, Marcel Dekker, Inc.

E. Dendy Sloan, J. (2003). "Fundamental Principles and Applications of Natural Gas Hydrates." Nature **Vol 426**.

Fu, B. (2002). The Development of Advanced Kinetic Hydrate Inhibitors. Chemistry in the oil industry IIV. T. Balson, H. A. Craddock, J. Dunlopet al. Cambridge, UK, Royal Society of Chemistry**:** 13.

Fu, B., C. Housten, et al. (2005). "New Generation LDHI with an Improved Environmental Profile." Proceedings of the Fifth International Conference on Gas Hydrates **4**: 11.

Gabitto, J. F. and C. Tsouris (2009). "Physical Properties of Gas Hydrates: A Review." Journal of Thermodynamics **2010, Article ID 271291**: 12.

Heidaryan, E., A. Salarabadi, et al. (2010). "A New High Performance Gas Hydrate Inhibitor." Journal of Natural Gas Chemistry **19**(3): 323-326.

Heroit-Watt-Institute-of-Petroleum-Engineering. (2011). "What are Gas Hydrates?", from http://www.pet.hw.ac.uk/research/hydrate/hydrates_what.cfm.

Huang, B., Y. Wang, et al. (2007). Natural Gas Chemistry **16**: 81.
Jussaume, L., J. P. Canselier, et al. (1999). Proceedings of the AICHE Spring National Meeting. Houston, Texas.
Kashchiev, D. and A. Firoozabadi (2002). "Induction Time in Crystallization of Gas Hydrates." Crystal Growth.
Kelland, M. A. (2006). "History of the Development of Low Dosage Hydrate Inhibitors." Energy&Fuels - An American Chemical Society Journal **20**(3).
Kelland, M. A. (2009). Production Chemicals For the Oil and Gas Industry. Boca Raton, Fla., CRC Press.
Kelland, M. A., T. M. Svartås, et al. (2008). "Gas Hydrate Anti-Agglomerant Properties of Polyproxylates and Some Other Demulsifiers." Journal of Petroleum Science and Engineering: 10.
Kelland, M. A., T. M. Svartås, et al. (1994). SPE 28506. Proceedings of the SPE 69th Annual Technical Conference and Exhibition. New Orleans, LA.
Kelland, M. A., T. M. Svartås, et al. (1995). Studies on New Gas Hydrate Inhibitors. SPE Offshore Europe Conference. Aberdeen.
Kelland, M. A., T. M. Svartås, et al. (2000). Experiments Related to the Performance of Gas Hydrate Kinetic Inhibitors. Proceedings of the 6th International Conference on Gas Hydrates, Annals of the New York Academy of Science. **912:** 744.
Kelland, M. A., T. M. Svartås, et al. (2000). "A New Class of Kinetic Hydrate Inhibitor." Annals of the New York Academy of Sciences **912: 281-293**.
Klomp, U. C. and A. P. Mehta (2007). Validation of Kinetic Inhibitors for Sour Gas Fields. International Petroleum Technology Conference. Dubai, U.A.E.
Koh, C. A., R. E. Westacott, et al. (2002). "Mechanisms of Gas Hydrate Formation and Inhibition." Fluid Phase Equilibria **194-197**: 9.
Kvenvolden, K. A. (1993). "Gas Hydrates - Geological Perspective and Global Change." Reviews of Geophysics **31**: 15.
Lee, J. D. and P. Englezos (2006). Chemical Engineering Science **61**: 1368-1376.
Lippmann, D., D. Kessel, et al. (1995). Proceedings of the 5th International Offshore and Polar Engineering Conference. The Hauge, The Netherlands.
Long, J., J. P. Lederhos, et al. (1994). Proceedings of the 73rd Annual GPA Convention. New Orleans, LA.
Lovell, D. and M. Pakulski (2003). "Two Low-Dasage Hydrate Inhibitors." Journal of petroleum technology **55**(4): 2.
Lund, A., D. E. Akporiaye, et al. (2004). Patent 6688180.
Lund, A., O. Urdahl, et al. (1996). Proceedings of the 2nd International COnference on Natural Gas Hydrates. Toulouse, France**:** 407-414.
Makogon, J. F. (1997). Hydrates of Hydrocarbons. Tulsa, Okla., PennWell Books.
Makogon, T. Y., R. Larsen, et al. (1997). Crystal Growth **179**: 258-262.
Mehta, A. P., P. B. Hebert, et al. (2002). "Fulfilling the Promise of Low Dosage Hydrate Inhibitors: Journey from academic curiosity to successful field implementation." OnePetro: 7.
Mullin, J. W. (2001). Crystallization 4th Edition. Amsterdam, Butterworth-Heinemann.
Ning, F., L. Zhang, et al. (2010). "Gas-Hydrate Formation, Agglomeration and Inhibition In Oil-Based Drilling Fluids for Deep-Water Drilling." Journal of Natural Gas Chemistry: 6.
Oskarsson, H., A. Lund, et al. (2005). Proceedings of the SPE International Symposium in Oilfield Chemistry. Houston, Texas**:** SPE 93075.

Oskarsson, H., I. Uneback, et al. (2005). "Evaluation of Anti-Agglomerants as Gas-Hydrate Dispersant using Multi-Cell Technology." Proceedings of the Fifth International Conference on Gas Hydrates **4**: 12.
Oskarsson, H., I. Uneback, et al. (2005). Proceedings of the Fifth International Conference on Gas Hydrates. Trondheim, Norway**:** 1283.
Pakulski, M. (1997). Proceedings of the SPE International Symposium on Oilfield Chemistry. Houston, Texas, SPE 37285.
PSL-Systemtechnik. (2011, 21.02.2011). "Research of Gas Hydrates with the Sapphire Rocking Cell." from http://www.psl-systemtechnik.de/sapphire_rocking_cell0.html?&L=1.
Reed, R. L., L. R. Kelley, et al. (1993). Proceedings of the 1st International Conference on Natural Gas Hydrates. New York**:** 430.
Sloan, E. D. (1995). U.S. Patent 5420370.
Sloan, E. D. (2011). Natural Gas Hydrates in Flow Assurance. Amsterdam, Elsevier.
Sloan, E. D. and C. A. Koh, Eds. (2008). Clathrate Hydrates of Natural Gases, CRC Press.
Sloan, E. D., S. Subramanian, et al. (1998). "Quantifying Hydrate Formation and Kinetic Inhibition." Ind. Eng. Chem. Res. **27**.
Stern, L. A., S. H. Kirdy, et al. (1996). "Peculiarities of Methane Clathrate Hydrate Formation and Solid-State Deformation, Including Possible Superheating of Water Ice." American Association for the Advancement of Science **273; 1765-1968**.
Talley, L. D., G. F. Mitchell, et al. (2000). Annals of the New York Academy of Sciences **912**: 214-321.
Urdahl, O., A. Lund, et al. (1995). Chemical Engineering Science **50**: 863-870.
Zeng, H., L. D. Wi, et al. 2002. Proceedings of the 4th International Conference on Natural Gas Hydrates. Yokohama, Japan.